Duration of Earthquakes, Comparison Between Ground Motion and Structural Motion

by

Michael J. O'Rourke
Rodolfo Serna
Robert U. Johnson

Report No. CE-82-3

Sponsored by National Science Foundation
Directorate for Applied Science and
Research Applications (ASRA)

Grant No. PFR-7902871

Department of Civil Engineering
Rensselaer Polytechnic Institute
Troy, New York 12181

May 1982

TABLE OF CONTENTS

CHAPTER 1

Duration of Strong Ground Motion

There have been several proposed definitions of strong ground motion duration. Duration has been defined in terms of the equivalent number of cycles for cyclic soil strength and liquefaction studies (10) as well as in terms of time (2,3,7,11,13). At the present, however, none is widely accepted as the "best" significant duration of seismic ground shaking for civil engineering applications. In this chapter, several of these ground motion durations, which are most relevant to the behavior of structures during earthquakes, are presented and compared. In subsequent chapters, these ground motion durations are compared with the time interval during which there is significant seismically induced structural motion.

1.1 Bracketed Duration; BOLT

One of the simplest definitions of duration of strong ground motion is "bracketed" duration proposed by Bolt (2). This duration is defined to be the elapsed time between the first and last excursion of the absolute value of ground acceleration above a predefined level. The predefined acceleration level is often taken as 5% of the acceleration due to gravity and this value will be used herein. Figure 1.1 shows the N90E component of ground acceleration

recorded at the basement level of Caltech's Millikan Library during the 1971 San Fernando Earthquake. The start of bracketed duration $(t_1)_{BOLT}$ occurs at the first excursion above the 0.05g level which is at 4.64 seconds for this accelerogram. Likewise, the end of bracketed duration $(t_2)_{BOLT}$ occurs at 15.41 sec which corresponds to the last excursion above the 0.05g level. Hence for this component, BOLT's duration, Δ_{BOLT}, equals 10.77 sec.

For a given earthquake, Δ_{BOLT} tends to decrease with distance from the source due to the attenuation of ground accelerations. If the peak ground acceleration of the record is less than 0.05g, Δ_{BOLT} equals zero. In this manner, Bolt's duration takes into account the level as well as the elapsed time of strong ground shaking.

1.2 Trifunac and Brady Duration

Another definition of strong ground motion duration is the time interval during which a specific fraction of the total cumulative energy of the earthquake arrives at a particular site. The Arias intensity I_A of an earthquake at a given time t is given by the following integral(1):

$$I_A(t) = \frac{\pi}{2g} \int_0^t a^2(\tau)\, d\tau \qquad (1)$$

where $a(\tau)$ is a component of the acceleration time history at the site and g is the acceleration due to gravity. If t_f is the length of the record, then $I_A(t_f)$ is the total Arias intensity of the earthquake.

Husid (5) suggested plotting the energy buildup of an accelerogram with time, normalizing it with respect to the total energy or:

$$h_A(t) = \frac{I_A(t)}{I_A(t_f)} \tag{2}$$

The graph of $h_A(t)$ versus time is known as a Husid Plot.

Trifunac and Brady (11) define strong ground motion duration as the time interval during which a specific fraction, usually 90%, of the cumulative energy arrives at the site. That is

$$\Delta_{TB} = (t_2)_{TB} - (t_1)_{TB} \tag{3}$$

where

$$h_A[(t_1)_{TB}] = 0.05$$

and

$$h_A[(t_2)_{TB}] = 0.95$$

This is illustrated in Figure 1.2 which presents the Husid plot for the N90E component of ground acceleration recorded at the

basement of Millikan Library during the 1971 San Fernando Earthquake. For this particular component $(t_1)_{TB}$ equals 4.83 sec, while the end of significant ground motion, $(t_2)_{TB}$, occurs at 22.35 sec. Hence, using Trifunac and Bradys method, the strong ground motion duration, for this component Δ_{TB} is 17.52 sec.

Other limits for the specific fraction of total cumulative energy have been proposed for use with the Trifunac and Brady approach. However, in this report the 90% value, that is from 5% to 95%, will be used exclusively.

Unlike Bolt's duration, described in Section 1.1, Trifunac and Bradys significant durations of ground motion for a particular event tends to increase with distance from the source. This is thought to be due to the increasing importance of surface waves for distant sites.

1.3 M^{c}Cann and Shah Duration

Strong ground motion duration as defined by M^{c}Cann and Shah (7) is derived from the cumulative rms acceleration function (CRF). CRF is defined as

$$CRF(t_n) = \frac{\sum_{J=1}^{n} a^2(t_j)}{n-1} \qquad (4)$$

where a(t) is a acceleration time history component. The end of the strong shaking $(t_2)_{MS}$ is defined as the time when the derivative of the CRF is last positive. The initial time $(t_1)_{MS}$ is evaluated by repeating the process with a reversed acceleration time history. The general procedure is illustrated in Figure 1.3. The duration of strong ground motion is then the difference between these two time values.

$$\Delta_{MS} = (t_2)_{MS} - (t_1)_{MS} \tag{5}$$

Hence, using the M^{c}Cann and Shah method, the duration of significant ground motion corresponds to the time interval during which the average cumulative rate of energy increases or remains constant.

1.4 BOND'S Duration

Bond et al. (3) defined the significant duration of the earthquake ground motions as the interval of time during which direct shear waves (S-waves) are arriving at the site. As Dobry, Idriss and Ng (4) pointed out, for earthquakes having moderate magnitudes, accelerograms recorded at rock sites are usually composed of three parts:

(1) an initial weak part corresponding to the arrival of P-waves;

(2) a strong middle portion associated with the arrival of S-waves and some P-waves and;

(3) a final part corresponding to the arrival of surface waves and indirect P and S-waves.

Bond used a moving window RMS acceleration $\bar{a}(t)$ in the horizontal plane

$$\bar{a}(t) = \frac{1}{\delta} \int_{t-\delta/2}^{t+\delta/2} (a_x^2(\tau) + a_y^2(\tau))\, d\tau \qquad (6)$$

where δ is the width of the moving time window, $a_x(\tau)$ and $a_y(\tau)$ are the two orthogonal horizontal ground acceleration components, in determining the beginning $(t_1)_{BOND}$ and end $(t_2)_{BOND}$ of the strong middle portion of the records. The Husid Plot and graphs of the variation with time of the principle directions of ground motion were also used in determining the times $(t_1)_{BOND}$ and $(t_2)_{BOND}$.

Bond's procedure is illustrated in Figure 1.4 which shows the moving window rms acceleration plot for the N90E component of the ground motion recorded at Milliken Library during the 1971 San Fernando earthquake. For this site, $(t_1)_{BOND}$ = 4.3 sec while $(t_2)_{BOND}$ = 12.2 sec. Hence, the significant ground motion duration using BOND's method, Δ_{BOND}, is 7.9 sec for this site.

Since Bond utilizes acceleration in the horizontal plane his procedure yields a strong ground motion duration for a site,

while Bolt's , Trifunac and Brady, and M^{C}Cann and Shah methods yield durations for a component of ground motion (generally either of the two orthogonal horizontal components per site).

1.5 Vanmarcke and Lai Duration

Vanmarcke and Lai (13) proposed a ground motion duration based upon the RMS ground acceleration and the peak ground acceleration. The ground motion duration is chosen such that the expected peak value of the assumed stationary Gaussian process, which is a function of the RMS value and the duration, matches the observed peak ground acceleration. Notice with the four previous ground motion durations (Bolt, Trifunac and Brady, M^{C}Cann and Shah, and Bond) the beginning and end of the strong shaking are specified. However with Vanmarcke and Lai's method, only the total duration is determined, while the beginning and end of the strong shaking are not determined. For this reason, Vanmarcke and Lai's procedure will not be considered in this report.

1.6 Comparison between Ground Motion Durations

Table 1.1 lists ground stations which recorded the 1971 San Fernando Earthquake. The beginning of strong ground motion, using the methods of Bolt, Trifunac and Brady, M^{C}Cann and Shah, and Bond, are listed in Table 1.2 for the San Fernando stations listed in Table

1.1. For the same records Tables 1.3 and 1.4 list the end of strong shaking and duration of strong shaking, respectively using the four methods mentioned previously. M^{c}Cann and Shah (7) have compared their duration, Δ_{MS}, with Δ_{BOLT} and Δ_{TB}. Bond's duration Δ_{BOND} could not have been included in this comparison since it was not available at the time of publication of ref. 7. M^{c}Cann and Shah conclude that Δ_{TB} is longer than Δ_{MS}. There is considerable scatter in the comparison between Δ_{BOLT} and Δ_{MS} with no general trend apparent. M^{c}Cann and Shah contend that this is probably due to the arbitrary choice of the cutoff acceleration level used. However, there is also an arbitrary choice involved in the Trifunac and Brady method (5% to 95% versus 10% to 90% for example). It seems reasonable to suspect that much of the scatter between Δ_{MS} and Δ_{BOLT} is due to the fact that, as mentioned previously, Δ_{BOLT} takes into consideration the level of ground shaking as well as its duration.

Bond's duration, Δ_{BOND}, ranges from 5 to 8 sec. for sites south of the San Fernando epicenter and from 3 to 4 seconds for sites north of the epicenter. These values are generally smaller than Δ_{TB} and Δ_{MS} for the same sites. There is no general trend between Δ_{BOND} and Δ_{BOLT}. Again, this is most likely due to the fact that Δ_{BOLT} takes into consideration the level of shaking.

As mentioned previously, Bolt's, Trifunac and Brady's, and M^{c}Cann and Shah's method yield two values for strong ground motion duration at a particular station (one for each of the two orthogonal horizontal components). Using these three methods, there is in general

fairly good agreement between the two ground motion durations for a particular site. That is, Δ_{TB} for the North-South component at a particular site is generally close in value to Δ_{TB} for the East-West component at the same site. This consistency among components also holds for both the start and the end of strong shaking, using any of the three methods.

Table 1.1 - Stations Recording the 1971 San Fernando Earthquake

CalTech Number	Building Name	Address	Accelerograph Locations
C048, C050	Holiday Inn	8244 Orion Blvd.	1st Floor, 8th Floor
C054, C055	Union Bank Square	445 Figueroa St.	Sub-basement, 19th Floor
D062, D064	Holiday Inn	1640 S. Marango St.	1st Floor, 8th Floor
E075, E077	Tishman Plaza	3470 Wilshire Ave.	Sub-basement, 11th Floor
E083, E085	Mutual Building	3407 Sixth St.	Basement, Penthouse
F089, F091	AMPCO Auto Park Ramp	808 S. Olive St.	Street Level, 8th Level
F095, F097	Robertson Plaza	120 N. Robertson Blvd.	Sub-basement, 9th Floor
F098, F100	Los Angeles Athletic Club, Parking Ramp	646 S. Olive St.	Basement, Roof
G108, G109	Millikan Library	Cal. Inst. of Tech.	Basement, 10th Floor
G112, G113	Crockers Bank Plaza	611 W. Sixth St.	Basement, 42nd Floor
H115, H117	Bank of California	15250 Ventura Blvd.	Basement, Roof
H118, H120	Airport Marina Hotel	8639 Lincoln Ave.	Basement, 12th Floor
H124, H126	Hunt Wessons Building	2600 Nutwood Ave.	Basement, Penthouse
I128, I130	Beverly Oakhurst Apartments	435 N. Oakhurst Ave.	Basement, Roof
I131, I133	450 Company	450 N. Roxbury Dr.	1st Floor, 10th Floor
I134, I136	Northrop	1800 Century Park East	Basement (P-3), Penthouse
I137, I139	Ventura Gloria Building	15190 Ventura Blvd.	Basement, 19th Floor
J145, J147	Valley Presbyterian Hospital	15107 Vanowen St.	Basement, Roof
J148, J150	Wilshire Christian Manor	616 S. Normandie Ave.	Basement, Roof

Table 1.1 - (continued)

CalTech Number	Building Name	Address	Accelerograph Locations
K157, K158	Pacific Telephone	420 S. Grand Ave.	2nd Floor, 17th Floor
L166, L168	Sheraton-Universal	3838 Lankershim Blvd.	Basement, 21st Floor
M176, M178	Occidental Center	1150 S. Hill St.	Sub-basement, 10th Floor
M180, M182	The City Center	4000 W. Chapman Ave.	Basement, 19th Floor
N188, N190	Property Research	1880 Century Park East	1st Level Parking, Penthouse
N192, N194	Wilshire-Coronado	2500 Wilshire Blvd.	Basement, Roof
O199, O201		1625 Olympic Blvd.	Ground Floor, 10th Floor
P214, P216	Kaiser Hospital	4867 Sunset Blvd.	Basement, 7th Floor
P217, P219	Wilshire Square	3345 Wilshire Blvd.	Basement, 12th Floor
Q233, Q235	Certified Life Tower	14724 Ventura Blvd.	1st Floor, Penthouse
Q236, Q238	Holiday Inn	1750 N. Orchid Ave.	Ground Floor, 23rd Floor
Q239, Q240	Wilshire Doheny Plaza	9100 Wilshire Blvd.	Basement, 5th Floor
Q241, Q243	Bunker Hill, Central Tower	800 W. First St.	1st Floor, 33rd Floor
R244, R245	Bunker Hill West Tower	222 Figueroa St.	1st Floor, 20th Floor
R246, R267		6464 Sunset Blvd.	Basement, 12th Floor
R249, R250		1900 Ave. of the Stars	Basement, 29th Floor
R251, R252	Bunker Hill, South Tower	234 Figueroa St.	Basement, Roof
R253, R254	Coldwell-Banker	535 S. Fremont Ave.	Basement, 6th Floor
S255, S257	6200 Wilshire Medical	6200 Wilshire Blvd.	Ground Floor

Table 1.1 - Continued

CalTech Number	Building Name	Address	Accelerograph Locations
S 258, S260	Phillips Hall, Univ. of So. Cal.	3440 University Ave.	Basement, Roof
S262, S264	Mutual Benefit Life Plaza	5900 Wilshire Blvd.	'B' Parking Lot, Penthouse
S267, S269	Airport Freeway Center	5260 Century Blvd.	1st Floor, Roof

TABLE 1.2

Start of Strong Ground Motion for Stations which Recorded the 1971 San Fernando Earthquake

CalTech Number	Direction	$(t_1)_{BOLT}$ (sec)	$(t_1)_{TB}$ (sec)	$(t_1)_{MS}$ (sec)	$(t_1)_{BOND}$ (sec)
C048	N00W	1.91	3.93	1.90	2.70
C048	S90W	2.65	3.01	2.60	2.70
C054	N52W	2.15	2.57	1.88	1.80
C054	S38W	2.02	2.37	1.90	1.80
D062	N38W	4.81	4.85	4.48	4.40
D062	S52W	4.49	4.71	4.54	4.40
E075	North	1.74	2.34	1.42	1.30
E075	East	1.62	1.72	1.40	1.30
E083	South	1.41	2.18	1.22	1.20
E083	East	1.32	1.55	1.18	1.20
F089	S53E	4.81	5.06	4.78	4.60
F089	S37W	4.95	4.99	4.50	4.60
F095	S88E	2.91	3.15	1.52	2.70
F095	S02W	3.67	3.66	2.42	2.70
F098	S53E	4.95	5.31	5.02	4.90
F098	S37W	4.99	5.53	4.94	4.90
G108	North	4.49	4.66	4.20	4.30
G108	East	4.64	4.83	4.20	4.30
G112	N38E	2.94	2.94	2.22	2.20
G112	N52W	3.12	2.78	2.36	2.20
H115	N11E	4.25	4.56	4.10	4.10
H115	N79W	4.11	4.90	4.12	4.10

TABLE 1.2

(continued)

CalTech Number	Direction	$(t_1)_{BOLT}$ (sec)	$(t_1)_{TB}$ (sec)	$(t_1)_{MS}$ (sec)	$(t_1)_{BOND}$ (sec)
H124	Center West	----	9.71	9.60	8.60
H124	Center South	----	9.85	9.52	8.60
I128	North	5.50	5.51	4.94	5.10
I128	West	5.53	5.51	1.44	5.10
I131	N50E	6.58	6.91	6.30	6.60
I131	N40W	6.43	6.82	6.10	6.60
I134	N54E	6.54	6.59	5.86	6.20
I134	S36E	6.65	6.58	5.86	6.20
I137	S81E	5.41	5.95	3.60	4.80
I137	S09W	5.11	6.15	3.50	4.80
J145	South	2.44	3.10	0.06	1.60
J145	West	1.82	2.92	1.14	1.60
J148	North	6.08	6.35	6.40	5.60
J148	West	5.90	6.00	5.80	5.60
K157	S53E	3.12	3.63	2.88	2.90
K157	S37W	3.34	3.36	1.92	2.90
L166	North	2.01	2.70	0.58	1.60
L166	West	1.77	2.22	0.78	1.60
M176	N37E	2.80	3.43	0.24	2.40
M176	S53W	2.62	2.89	0.26	2.40
M180	South	----	2.70	1.44	1.50
M180	West	----	2.83	1.44	1.50
N188	N54E	6.29	6.33	5.64	5.70
N188	N36W	5.63	6.11	5.64	5.70
N192	N29E	4.50	4.51	0.66	4.10
N192	N61W	4.59	4.69	4.20	4.10
0199	N28E	7.06	7.20	4.16	6.50
0199	N62W	6.61	7.20	6.64	6.50

TABLE 1.2
(continued)

CalTech Number	Direction	$(t_1)_{BOLT}$ (sec)	$(t_1)_{TB}$ (sec)	$(t_1)_{MS}$ (sec)	$(t_1)_{BOND}$ (sec)
P214	S89W	1.12	1.52	0.62	1.10
P214	S01E	1.33	1.58	0.90	1.10
P217	South	2.15	2.14	1.34	1.20
P217	East	1.48	1.59	1.34	1.20
Q233	S12W	5.02	5.23	5.12	4.90
Q233	N78W	4.81	5.43	4.90	4.90
Q236	South	4.93	5.25	4.86	4.80
Q236	East	5.36	4.84	4.46	4.80
Q239	South	5.15	5.33	4.90	5.00
Q239	East	5.19	5.45	5.14	5.00
Q241	N37E	6.63	6.80	6.56	6.30
Q241	N53W	6.77	6.80	6.34	6.30
R244	N53W	5.67	5.92	5.48	5.50
R244	S37W	5.84	6.14	5.88	5.50
R246	South	5.73	5.77	5.34	5.10
R246	East	5.30	5.67	5.36	5.10
R249	N44E	5.55	5.51	4.84	5.10
R249	S46E	5.38	5.42	5.04	5.10
R251	N37E	3.36	4.14	3.48	3.20
R251	S53W	3.54	3.77	3.14	3.20
R253	N30W	6.22	6.49	6.18	5.90
R253	S60W	6.06	6.57	6.18	5.90
S255	N08E	1.19	1.44	1.12	1.10
S255	N82W	1.28	1.79	1.30	1.10
S258	N29E	10.07	6.52	6.08	6.60
S258	S71E	9.78	6.77	5.50	6.60
S262	N83W	3.65	2.85	2.28	2.00
S262	S07W	4.74	3.28	2.52	2.00
S267	North	17.19	6.98	6.68	6.30
S267	East	7.70	7.68	6.72	6.30

TABLE 1.3

End of Strong Ground Motion for Stations which Recorded the 1971 San Fernando Earthquake

CalTech Number	Direction	$(t_2)_{BOLT}$ (sec)	$(t_2)_{TB}$ (sec)	$(t_2)_{MS}$ (sec)	$(t_2)_{BOND}$ (sec)
C048	N00W	20.57	20.52	14.70	——
C048	S90W	20.59	24.67	20.60	——
C054	N52W	8.84	15.81	7.68	7.70
C054	S38W	12.05	18.23	12.10	7.70
D062	N38W	14.80	18.20	11.08	11.30
D062	S52W	12.41	16.91	11.14	11.30
E075	North	14.57	17.66	14.22	7.60
E075	East	12.17	17.32	12.20	7.60
E083	South	13.74	15.06	7.62	7.80
E083	East	13.94	14.80	9.98	7.80
F089	S53E	11.33	17.74	10.58	10.60
F089	S37W	14.71	20.70	14.90	10.60
F095	S88E	8.80	22.65	19.42	9.00
F095	S02W	9.64	27.71	14.88	9.00
F098	S53E	16.15	17.69	10.62	10.90
F098	S37W	15.24	18.22	10.54	10.90
G108	North	14.84	17.79	8.60	12.20
G108	East	15.41	22.35	9.80	12.20
G112	N38E	9.29	17.07	9.22	8.00
G112	N52W	10.54	18.65	13.36	8.00
H115	N11E	21.08	23.00	18.18	9.70
H115	N79W	22.28	29.44	22.36	9.70

TABLE 1.3

(continued)

CalTech Number	Direction	$(t_2)_{BOLT}$ (sec)	$(t_2)_{TB}$ (sec)	$(t_2)_{MS}$ (sec)	$(t_2)_{BOND}$ (sec)
H124	Center West	-----	31.23	32.60	-----
H124	Center South	-----	30.73	32.92	-----
I128	North	10.46	20.28	22.42	13.00
I128	West	12.84	19.49	21.26	13.00
I131	N50E	14.31	19.20	12.70	12.80
I131	N40W	14.98	24.09	12.50	12.80
I134	N54E	13.04	31.34	13.06	13.00
I134	S36E	12.65	37.19	12.66	13.00
I137	S81E	24.91	32.40	35.90	-----
I137	S09W	21.24	27.97	36.10	-----
J145	South	18.18	29.36	25.86	-----
J145	West	24.48	31.14	24.74	-----
J148	North	18.45	18.21	18.40	13.20
J148	West	16.23	16.20	16.20	13.20
K157	S53E	9.74	17.16	8.68	8.70
K157	S37W	9.14	19.03	13.12	8.70
L166	North	8.70	14.60	10.30	7.50
L166	West	8.00	14.26	7.66	7.50
M176	N37E	13.38	21.04	14.72	10.20
M176	S53W	11.41	18.27	17.46	10.20
M180	South	-----	77.06	55.10	7.80
M180	West	-----	71.84	86.56	7.80
N188	N54E	12.64	28.97	12.24	12.80
N188	N36W	17.28	23.12	12.64	12.80
N192	N29E	14.40	18.37	18.52	11.00
N192	N61W	10.70	16.35	17.60	11.00
O199	N28E	16.84	21.86	23.50	12.90
O199	N62W	14.60	19.29	36.12	12.90

TABLE 1.3
(continued)

CalTech Number	Direction	$(t_2)_{BOLT}$ (sec)	$(t_2)_{TB}$ (sec)	$(t_2)_{MS}$ (sec)	$(t_2)_{BOND}$ (sec)
P214	S89W	9.13	11.07	9.14	7.20
P214	S01E	7.19	12.15	7.18	7.20
P217	South	7.76	16.76	14.14	7.90
P217	East	7.62	15.86	11.94	7.90
Q233	S12W	22.56	21.67	15.52	10.80
Q233	N78W	27.90	28.04	27.90	10.80
Q236	South	14.43	17.51	10.46	10.70
Q236	East	10.55	18.63	10.66	10.70
Q239	South	16.82	20.24	11.30	12.20
Q239	East	13.17	21.12	13.14	12.20
Q241	N37E	14.24	21.88	16.76	12.40
Q241	N53W	16.77	21.22	14.14	12.40
R244	N53W	13.85	19.74	11.08	11.20
R244	S37W	9.54	21.21	14.28	11.20
R246	South	14.85	21.80	14.94	10.80
R246	East	16.02	19.90	15.36	10.80
R249	N44E	11.39	32.32	11.44	11.80
R249	S46E	11.69	29.01	16.04	11.80
R251	N37E	10.46	15.46	12.68	10.20
R251	S53W	13.13	18.53	8.74	10.20
R253	N30W	14.64	17.09	11.98	12.10
R253	S60W	17.96	17.95	11.98	12.10
S255	N08E	7.68	18.35	5.52	7.00
S255	N82W	9.81	18.43	14.30	7.00
S258	N29E	14.27	24.40	16.48	12.00
S258	S71E	11.52	25.94	20.90	12.00
S262	N83W	14.61	21.71	20.68	8.70
S262	S07W	16.89	18.01	17.12	8.70
S267	North	17.54	32.83	25.28	----
S267	East	12.25	40.20	41.12	----

TABLE 1.4

Duration of Strong Ground Motion for Stations which Recorded the 1971 San Fernando Earthquake

CalTech Number	Direction	Δ_{BOLT} (sec)	Δ_{TB} (sec)	Δ_{MS} (sec)	Δ_{BOND} (sec)
C048	N00W	18.66	16.59	12.80	----
C048	S90W	17.94	21.66	18.00	----
C054	N52W	6.69	13.24	5.80	5.90
C054	S38W	10.03	15.86	10.20	5.90
D062	N38W	9.99	13.35	6.60	6.90
D062	S52W	7.92	12.20	6.60	6.90
E075	North	12.83	15.32	12.80	6.30
E075	East	10.55	15.60	10.80	6.30
E083	South	12.33	12.88	6.40	6.60
E083	East	12.62	13.25	8.80	6.60
F089	S53E	6.52	12.68	5.80	6.00
F089	S37W	9.77	15.71	10.40	6.00
F095	S88E	5.89	19.50	17.90	6.30
F095	S02W	5.97	24.05	12.46	6.30
F098	S53E	11.19	12.38	5.60	6.00
F098	S37W	10.25	12.69	5.60	6.00
G108	North	10.34	13.14	4.40	7.90
G108	East	10.77	17.52	5.60	7.90
G112	N38E	6.35	14.13	7.00	5.80
G112	N52W	7.42	15.87	11.00	5.80
H115	N11E	16.83	18.44	14.08	5.60
H115	N79W	18.17	24.54	18.24	5.60
H124	Center West	0.0	21.52	23.00	----
H124	Center South	0.0	20.88	23.40	----
I128	North	4.96	14.77	17.48	7.90
I128	West	7.31	13.98	19.82	7.90

TABLE 1.4

(continued)

CalTech Number	Direction	Δ_{BOLT} (sec)	Δ_{TB} (sec)	Δ_{MS} (sec)	Δ_{BOND} (sec)
I131	N50E	7.73	12.29	6.40	6.20
I131	N40W	8.55	17.27	6.40	6.20
I134	N54E	6.50	24.76	7.20	6.80
I134	S36E	5.99	30.61	6.80	6.80
I137	S81E	19.50	26.45	32.30	----
I137	S09W	16.13	21.82	32.60	----
J145	South	15.74	26.26	25.80	----
J145	West	22.66	28.22	23.60	----
J148	North	12.38	11.86	12.00	7.60
J148	West	10.34	10.20	10.40	7.60
K157	S53E	6.63	13.53	5.80	5.80
K157	S37W	5.80	15.67	11.20	5.80
L166	North	6.68	11.90	9.72	5.90
L166	West	6.23	12.04	6.88	5.90
M176	N37E	10.48	17.61	14.48	7.80
M176	S53W	8.79	15.38	17.20	7.80
M180	South	0.0	74.36	53.88	6.30
M180	West	0.0	69.01	85.12	6.30
N188	N54E	6.35	22.64	6.60	7.10
N188	N36W	11.56	17.01	7.00	7.10
N192	N29E	9.90	13.86	17.86	6.90
N192	N61W	6.11	11.66	13.40	6.90
O199	N28E	9.78	14.66	19.34	6.40
O199	N62W	7.99	12.09	29.48	6.40
P214	S89W	8.03	9.55	8.52	6.10
P214	S01E	5.86	10.57	6.28	6.10

TABLE 1.4

(continued)

CalTech Number	Direction	Δ_{BOLT} (sec)	Δ_{TB} (sec)	Δ_{MS} (sec)	Δ_{BOND} (sec)
P217	South	5.61	14.62	12.80	6.70
P217	East	6.14	14.27	10.60	6.70
Q233	S12W	17.54	16.44	10.40	5.90
Q233	N78W	23.08	22.61	23.00	5.90
Q236	South	9.50	12.26	5.60	5.90
Q236	East	5.20	13.79	6.20	5.90
Q239	South	11.67	14.91	6.40	7.20
Q239	East	7.98	15.67	8.00	7.20
Q241	N37E	7.61	15.08	10.20	6.10
Q241	N53W	10.00	14.42	7.80	6.10
R244	N53W	8.17	13.82	5.60	5.70
R244	S37W	15.38	15.07	19.40	5.70
R246	South	9.11	16.03	9.60	5.70
R246	East	10.72	14.23	10.00	5.70
R249	N44E	5.84	26.81	6.60	6.70
R249	S46E	6.31	23.59	11.00	6.70
R251	N37E	7.10	11.32	9.20	7.00
R251	S53W	9.59	14.76	5.60	7.00
R253	N30W	8.41	10.60	5.80	6.20
R253	S60W	11.90	11.38	5.80	6.20
S255	N08E	6.48	16.91	4.40	5.90
S255	N82W	8.53	16.64	13.00	5.90
S258	N29E	4.17	17.81	10.40	5.40
S258	S71E	2.74	19.17	15.40	5.40
S262	N83W	10.97	18.86	18.40	6.70
S262	S07W	12.15	14.73	14.60	6.70
S267	North	0.35	25.85	18.60	----
S267	East	4.56	35.79	34.40	----

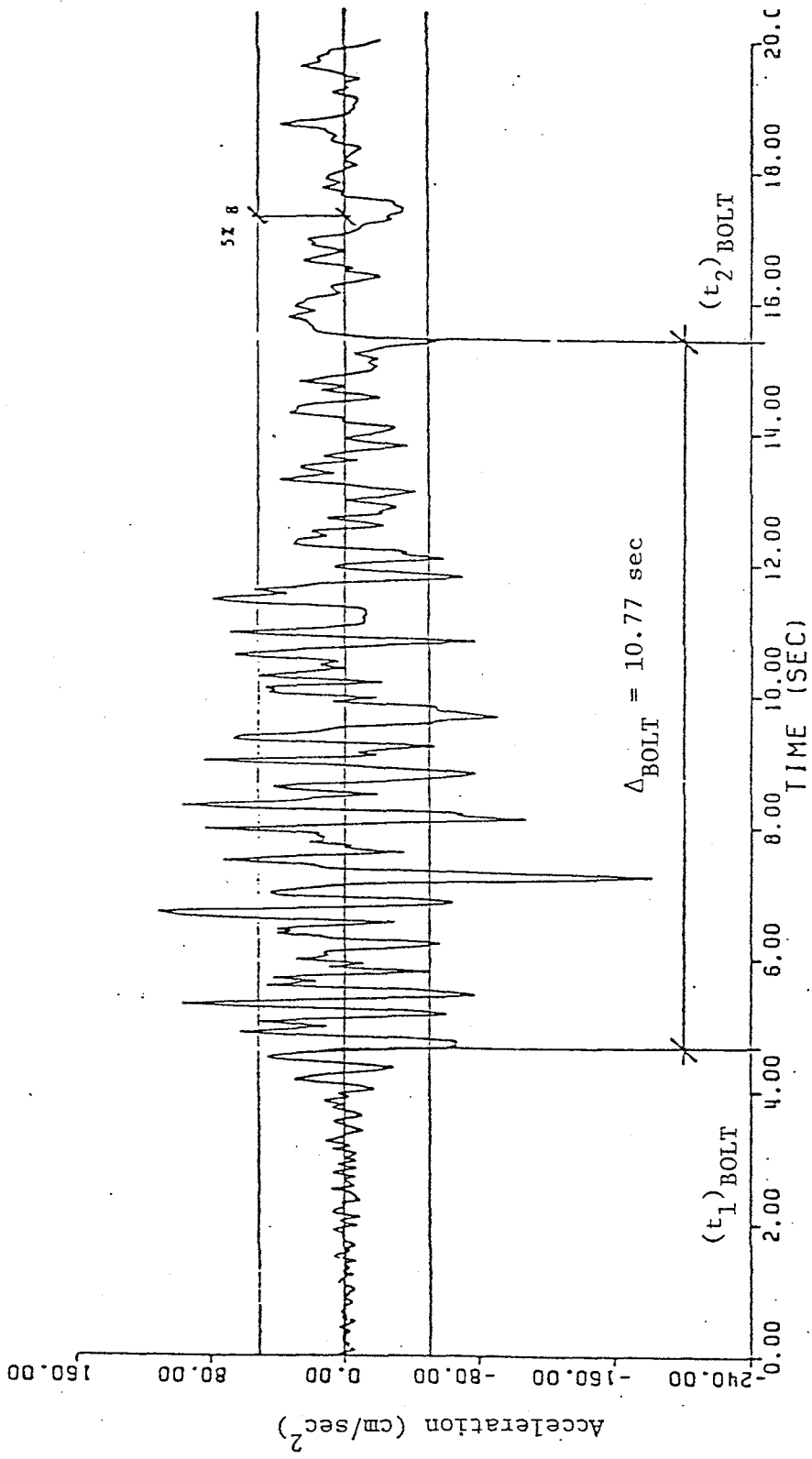

Figure 1.1 N90E Ground Acceleration Component of Millikan Library during 1971 San Fernando Earthquake Showing Bolts Duration

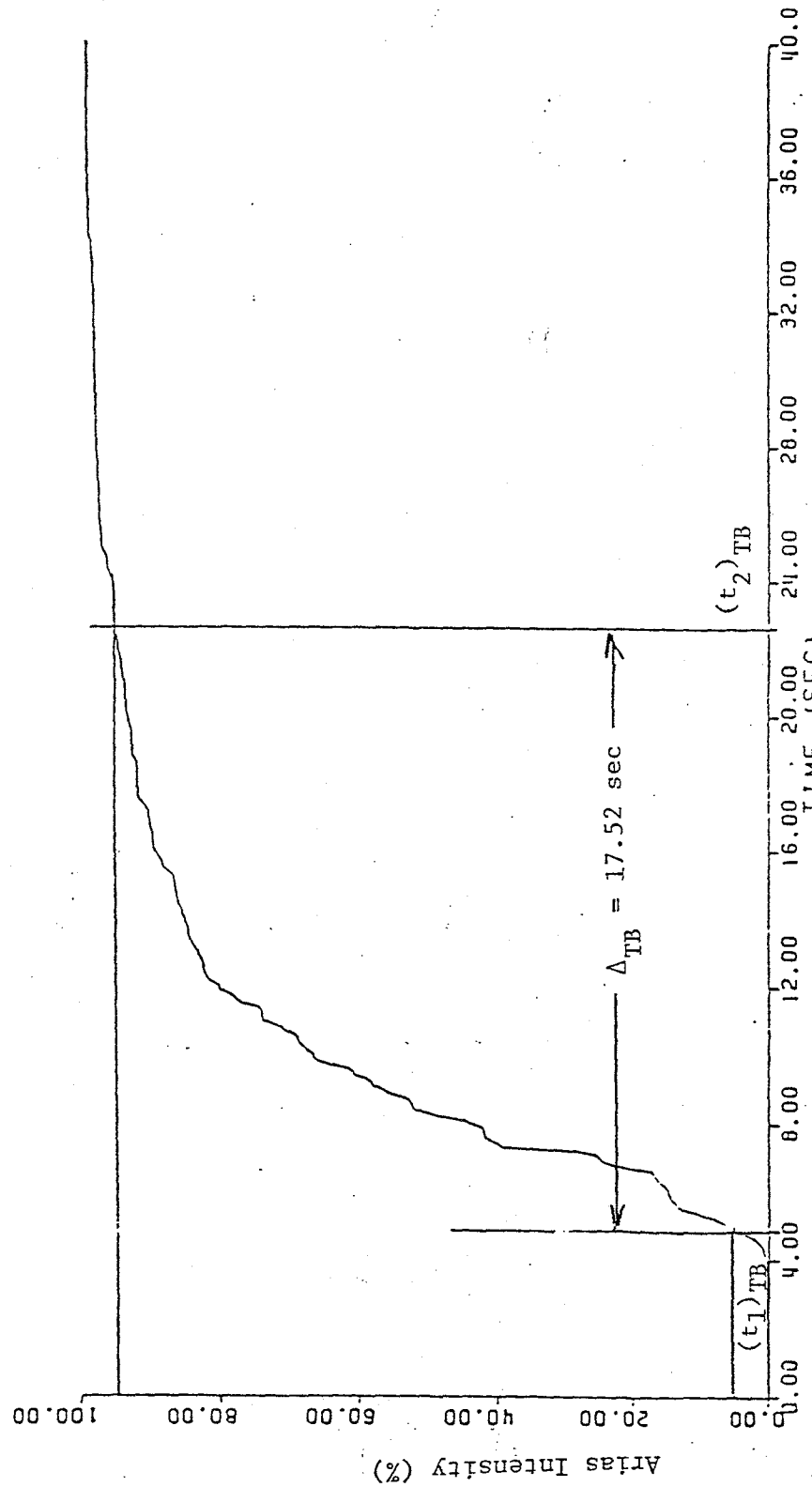

Figure 1.2 Husid Plot for N90E Ground Acceleration Component at Millikan Library During the 1971 San Fernando Earthquake, Showing Trifunac and Brady Duration

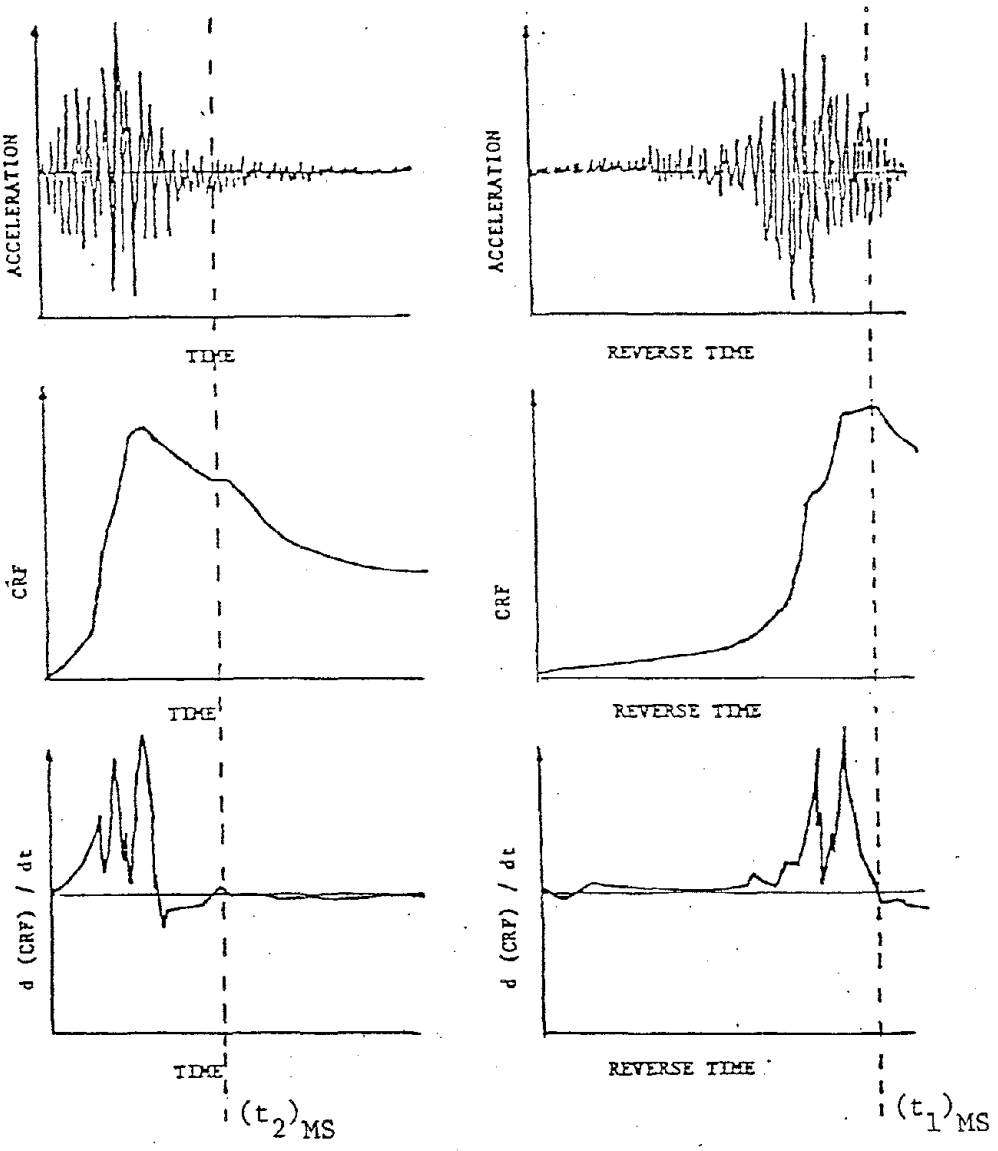

Figure 1.3 Illustration of M^{c}Cann and Shah Significant Duration

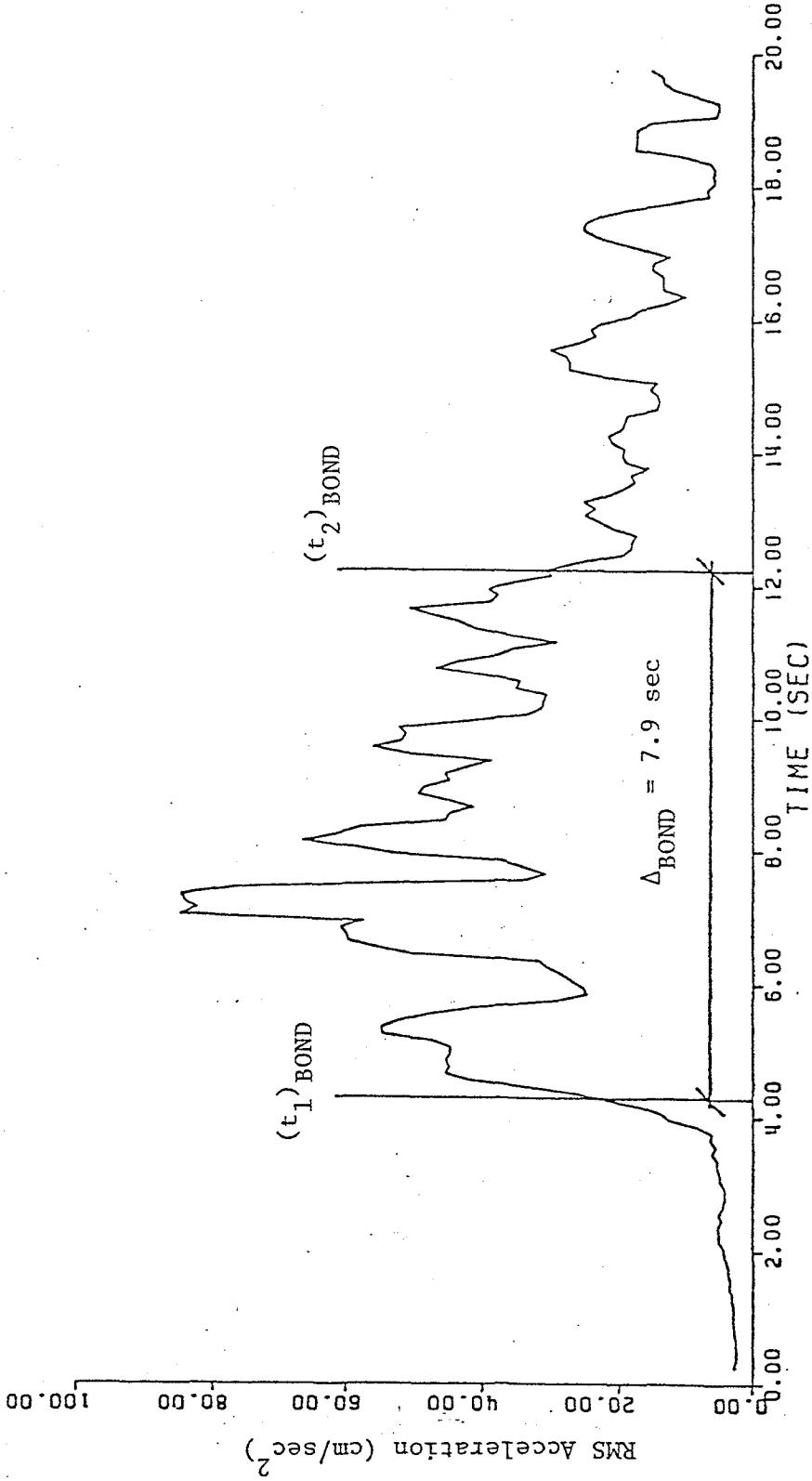

Figure 1.4 Moving Time Window RMS Acceleration for N90E Component At Millikan Library During 1971 San Fernando Earthquake, Showing Bonds Duration

CHAPTER 2

Duration of Strong Structural Response

In the previous chapter, several definiations of the duration strong ground motion due to earthquakes were presented and compared. It was found, in general, that $\Delta_{TB} \geq \Delta_{MS} \geq \Delta_{BOND}$. There was no apparent trend for Δ_{BOLT}. This is likely due to the fact that Bolt's method takes into consideration the level or amplitude of ground motion. It is worth noting that the strong ground motion durations due to Bolt, Trifunac and Brady, and M^{c}Cann and Shah are all calculated directly from an acceleration time history of the ground motion. Bond's methods utilizes the acceleration time history as well as other ground motion characteristics such as the principal direction of ground motion.

In this chapter, the time period during which the relative displacements in structures subjected to earthquake ground motion are largest, are determined. These durations of strong structural response are then compared to the strong ground motion duration.

2.1 Duration of Strong Structural Motion Based on Relative Displacement

The various ground motion durations considered herein attempt to quantify the most significant portion of the ground acceleration time history. For structures, the most important response parameter is the

relative interstory displacements. The strains and hence stresses in the structures lateral load resisting system are directly related to these interstory displacements. Most of the available records of structural response to earthquakes consist of the acceleration, velocity and displacement of the top and basement or ground levels of the structure. For all the structures listed in Table 1.1, these ground and top of building records are available for the 1971 San Fernando Earthquake. Hence, the relative displacement of the top floor with respect to the basement will be used herein as the response parameter of interest. Note that if the structure vibrates in its first mode only, the interstory displacements are proportional to the relative displacement between the top and basement levels.

The procedure used herein to determine the duration of strong structural response is based upon Trifunac and Brady's procedure for ground motion. The duration of strong structural response is defined as the time interval during which a Husid Plot for the relative displacement between the top and basement levels increases from 5% to 95% of its final value. That is,

$$\Delta_S = (t_2)_s - (t_1)_s \tag{7}$$

where

$$h_s[(t_1)_s] = 0.05$$

$$h_s[(t_2)_s] = 0.95$$

$$h_s(t) = \frac{\int_o^t x_r^2(\tau)\, d\tau}{\int_o^{t_f} x_r^2(\tau)\, d\tau} \qquad (8)$$

and $x_r(t)$ is the relative displacement of the top level of the structure with respect to its base and t_f is the total length of the record.

Figure 2.1 presents the relative displacement Husid Plot, $h_s(t)$, for the N90E component recorded at the Millikan Library during the 1971 San Fernando Earthquake. Note that $h_s(7.97) = 0.05$ while $h_s(28.42) = 0.95$. Hence $(t_1)_s = 7.97$ sec and $(t_2)_s = 28.42$ sec, and the duration of strong structural response for this component, Δ_s, equals 20.45 seconds.

Table 2.1 lists the beginning, end and duration of strong structural response for the structures in Table 1.1. In addition, Table 2.1 presents the predominant natural period, T, in both horizontal directions for the same group of structures. These predominant natural periods were taken as those exhibited by the structure "during" the 1971 San Fernando Earthquake and were calculated from information provided by Mulhern and Maley (8).

Unlike the duration of strong ground motion, one would expect that the duration of strong structural response may be related in some manner to the natural period of the structure. Presented in Figure 2.2 is a plot of the duration of strong structural response,

Δ_S, versus the predominate period of the structure, T. The structural durations are all larger than 10 sec. for the San Fernando event, otherwise there seems to be no correlation between the two variables.

Figure 2.3 presents a plot of the duration of strong structural response divided by the duration of strong ground motion versus the natural period of the structure. For this plot Δ_{TB} was used as the duration of strong ground motion. Δ_S/Δ_{TB} is generally larger than one, otherwise there seems to be little correlation between this ratio and the predominant period.

2.2 Comparison of Strong Structural Response with Strong Ground Motion

Figures 2.4 through 2.7 present graphs of the beginning of strong structural response, $(t_1)_S$, versus the beginning of strong ground motion $(t_1)_{BOLT}$, $(t_1)_{TB}$, $(t_1)_{MS}$, and $(t_1)_{BOND}$. Note that the vast majority of points, for all four ground motion procedures, fall above the one to one match line. This indicates that the start of strong structural response begins after the start of strong ground motion, as one might expect.

Figures 2.8 through 2.11 present graphs of the end of strong structural response, $(t_2)_S$ versus the end of strong ground motion $(t_2)_{BOLT}$, $(t_2)_{TB}$, $(t_2)_{MS}$, and $(t_2)_{BOND}$. Note that the vast majority of points, for all four ground motion procedures, again fall

above the one to one match line. This indicates that strong structural response continues after the strong ground motion has ended.

Figures 2.12 through 2.15 present graphs of the duration of strong structural response, Δ_S, versus the duration of strong ground motion Δ_{BOLT}, Δ_{TB}, Δ_{MS} and Δ_{BOND}. Inspection of the figures indictes that the duration of strong structural response is, in general, longer than the duration of strong ground motion.

No doubt some of the differences between the duration of strong ground motion and the duration of strong structural response are due to the relatively low damping ratios typical to buildings. That is, in certain cases the time interval between the end of strong ground motion and the end of strong structural response corresponds to lightly damped, quasi-free vibration.

Low structural damping, however, is not the only effect. Figure 2.16 presents a graph of $(t_1)_S-(t_1)_{BOND}$ versus the natural period of the structure. Recall that $(t_1)_{BOND}$ is the time of the first S-wave arrival at the site and that the other three starting times, $(t_1)_{BOLT}$, $(t_1)_{MS}$, and $(t_1)_{TB}$ are generally within a second or two of $(t_1)_{BOND}$. Although there is quite a bit of scatter, the figure indicates that the time interval between the arrival of the initial S-wave and the start of strong structural response is a function of the natural period T. For shorter period, higher frequency structures (i.e., T < 2 sec) the start of strong structural response occurs generally within 3 or 4 seconds of the arrival of S!.

However, for the longer period, lower frequency structures (i.e., $T \geq 2$ sec) the start of strong structural response can lag behind the start of strong ground motion by as much as 20 sec.

The same general conclusions can be drawn from Table 2.2 which present the mean and standard deviation of the difference between the start of strong ground motion, by each of the four methods, and the start of strong structural response. Table 2.3 presents a similar comparison for the end times. Listed in Table 2.4 are the mean and standard deviation of the ratio between strong ground motion duration and strong structural response duration. The means and standard deviations are presented separately for structures with $T < 2$ sec. and for structures with $T < 2$ sec, as well as for all structures. Notice for the shorter period structures, that, on the average, strong structural response begins about 2 seconds after the start of strong ground motion. Also strong structural response ends, on the average, about 15 seconds after the end of strong ground motion for these shorter period structures.

On the other hand, for the longer period structures, strong structural response begins, on the average, about 7.5 seconds after the start of strong ground motion. As a matter of fact, using Bolts, M^{C}Cann and Shah, and Bonds procedures, strong ground motion ends before strong structural response begins for many of these longer period structures. Strong structural response ends, again on the average, about 24 seconds after the end of strong ground motion for these longer period structures.

These differences are likely due to the fact that all the ground motion durations studied in this report are based upon ground accelerations. On the other hand, the motions of buildings, particularly those above 10 or 20 stories in height, tend to be more closely related to lower frequency ground velocities as opposed to higher frequency ground accelerations. That is, strong ground motion, based upon ground accelerations and generally corresponding to the S-wave arrivals, tends to coincide with strong structural response for shorter period structures. However, for longer period structures, strong ground motion based on acceleration does not coincide with strong structural response. For the latter, strong ground motion based upon ground velocities may be more appropriate. From the viewpoint of velocities, the later arrivals which include in many cases a strong surface wave contribution have an increased importance.

For the shorter period structures, the start of strong ground motion by any of the four methods is a fairly good estimate for the start of strong structural response. From Table 2.4 for T < 2 sec, the ratio Δ_g/Δ_s is closer to one for Trifunac and Brady's procedure Hence, Trifunac and Brady's procedure for the time period of strong ground motion matches best the time period of strong structural response for shorter period structures. On the otherhand, for longer period structur es, none of the four ground motion procedures match the time period during which strong structural response occurs.

TABLE 2.1

Start, End and Duration of Strong Structural Response and Natural Period of San Fernando Structures

CalTech Number	Direction	T (sec)	$(t_1)_S$ (sec)	$(t_2)_S$ (sec)	Δ_S (sec)
C048	N00W	1.67	10.81	33.64	22.83
C048	S90W	1.23	6.80	38.71	31.91
C054	N52W	3.51*	7.52	48.07	40.55
C054	S38W	3.33*	11.45	38.71	27.27
D062	N38W	1.03	5.44	25.72	20.79
D062	S52W	1.17	5.79	18.31	12.53
E075	North	1.59	5.90	33.18	27.28
E075	East	1.30	2.78	25.97	23.19
E083	South	1.59	5.00	31.31	26.32
E083	East	1.41	3.41	16.27	12.87
F089	S53E	0.40	0.51	25.83	25.31
F089	S37W	0.60	0.40	25.75	25.36
F095	S88E	0.60	3.38	38.37	34.99
F095	S02W	0.80	4.53	39.28	34.75
F098	S53E	0.30	5.52	38.32	32.80
F098	S37W	0.60	5.45	28.48	23.03
G108	North	0.67	5.96	25.12	19.15
G108	East	1.00	7.87	28.50	20.63
G112	N38E	5.88	6.05	35.68	29.64
G112	N52W	5.55	6.56	39.36	32.80
H115	N11E	2.38	16.14	36.36	20.22
H115	N79W	2.94	21.58	38.42	16.84
H124	Center West	0.70	12.30	33.82	21.52
H124	Center South	0.80	11.38	33.45	22.08
I128	North	0.60	6.94	21.00	14.06
I128	West	0.40	6.09	20.93	14.84

TABLE 2.1

(continued)

CalTech Number	Direction	T (sec)	$(t_1)_S$ (sec)	$(t_2)_S$ (sec)	Δ_S (sec)
I131	N50E	0.50	7.10	25.09	17.99
I131	N40W	0.80	7.15	33.21	26.06
I134	N54E	1.54	9.59	35.45	25.86
I134	S36E	1.04	7.70	33.93	26.23
I137	S81E	2.77	15.97	42.46	26.49
I137	S09W	3.22	13.42	42.05	28.63
J145	South	1.00	5.86	28.20	22.34
J145	West	0.90	3.98	35.04	31.06
J148	North	1.09	9.87	36.34	26.47
J148	West	1.78	8.94	32.57	23.63
K157	S53E	1.00	4.83	28.27	23.44
K157	S37W	1.00	4.09	23.24	19.15
L166	North	2.08	4.69	42.86	38.17
L166	West	2.27	4.96	32.89	27.93
M176	N37E	2.63	9.21	54.34	45.12
M176	S53W	2.50	5.96	64.74	58.77
M180	South	2.04	13.06	74.64	61.59
M180	West	1.13	8.70	66.99	58.29
N188	N54E	3.45	13.01	50.94	37.92
N188	N36W	2.94	15.98	43.65	27.67
N192	N29E	2.32	7.17	20.94	13.76
N192	N61W	1.88	8.83	24.03	15.20
O199	N28E	1.30	10.51	29.27	18.76
O199	N62W	1.40	8.52	38.43	29.91
P214	S89W	0.50	1.48	25.97	24.49
P214	S01E	0.40	1.88	22.01	20.13
P217	South	1.20	4.23	25.18	19.95
P217	East	1.00	3.09	19.06	15.97

TABLE 2.1

(continued)

CalTech Number	Direction	T (sec)	$(t_1)_S$ (sec)	$(t_2)_S$ (sec)	Δ_S (sec)
Q233	S12W	1.07	7.68	32.17	24.49
Q233	N78W	1.13	9.47	36.18	26.71
Q236	South	1.92	1.25	31.28	30.03
Q236	East	2.12	5.86	24.82	18.96
Q239	South	1.69	8.78	32.75	23.96
Q239	East	1.78	5.57	34.92	29.36
Q241	N37E	3.33	16.70	55.62	38.92
Q241	N53W	2.32	16.06	42.60	26.54
R244	N53W	1.10	8.29	25.46	17.17
R244	S37W	0.60	6.42	26.90	20.48
R246	South	2.32	8.45	27.49	19.04
R246	East	2.70	8.92	25.26	16.33
R249	N44E	3.44*	12.55	38.04	25.49
R249	S46E	3.44*	25.57	38.46	12.89
R251	N37E	1.20	3.93	27.78	23.85
R251	S53W	0.70	3.43	21.97	18.54
R253	N30W	1.10	9.37	33.93	24.56
R253	S60W	0.70	7.41	45.77	38.36
S255	N08E	1.49	4.01	39.10	35.09
S255	N82W	1.69	5.84	35.99	30.15
S258	N29E	1.00	10.08	24.48	14.40
S258	S71E	0.90	8.67	26.95	18.28
S262	N83W	5.0	10.04	24.03	13.99
S262	S07W	5.0	14.78	25.00	10.22
S267	North	2.08	12.49	43.78	31.29
S267	East	1.79	13.99	44.19	30.21

* Taken as average of "pre" and "post" earthquake periods from Ref. (8)

TABLE 2.2

Mean and Standard Deviation of Time Interval Between
Start of Strong Ground Motion and Start of Strong Structural Response

		$(t_1)_S - (t_1)_g$		
		T < 2 sec	T > 2 sec	All
Bolt	Mean	1.73	6.80	3.40
	St. Dev.	2.28	5.17	4.24
Trifunac & Brady	Mean	1.70	7.20	3.44
	St. Dev.	2.18	4.53	4.04
M^{c}Cann & Shah	Mean	2.61	8.30	4.42
	St. Dev.	2.54	4.38	4.18
Bond	Mean	2.24	7.89	4.08
	St. Dev.	2.32	4.57	4.18

TABLE 2.3

Mean and Standard Deviation of Time Interval Between
End of Strong Ground Motion and End of Strong Structural Response

		$(t_2)_S - (t_2)_g$		
		T < 2 sec	T > 2 sec	All
Bolt	Mean	16.01	24.7	18.9
	St. Dev.	6.68	11.7	9.57
Trifunac & Brady	Mean	8.78	16.3	11.2
	St. Dev.	6.69	11.4	9.16
M^{c}Cann & Shah	Mean	13.8	22.8	16.6
	St. Dev.	9.16	12.2	11.0
Bond	Mean	19.5	30.4	23.1
	St. Dev.	8.74	13.0	11.6

TABLE 2.4

Mean and Standard Deviation of Ratio Between
Strong Ground Motion and Strong Structural Response Durations

		$\Delta g/\Delta S$		
		T < 2 sec	T > 2 sec	All
Bolt	Mean	.385	.423	.397
	St. Dev.	.217	.308	.250
Trifunac & Brady	Mean	.732	.783	.748
	St. Dev.	.240	.407	.304
M^{C}Cann & Shah	Mean	.559	.586	.567
	St. Dev.	.338	.412	.364
Bond	Mean	.297	.270	.288
	St. Dev.	.103	.140	.117

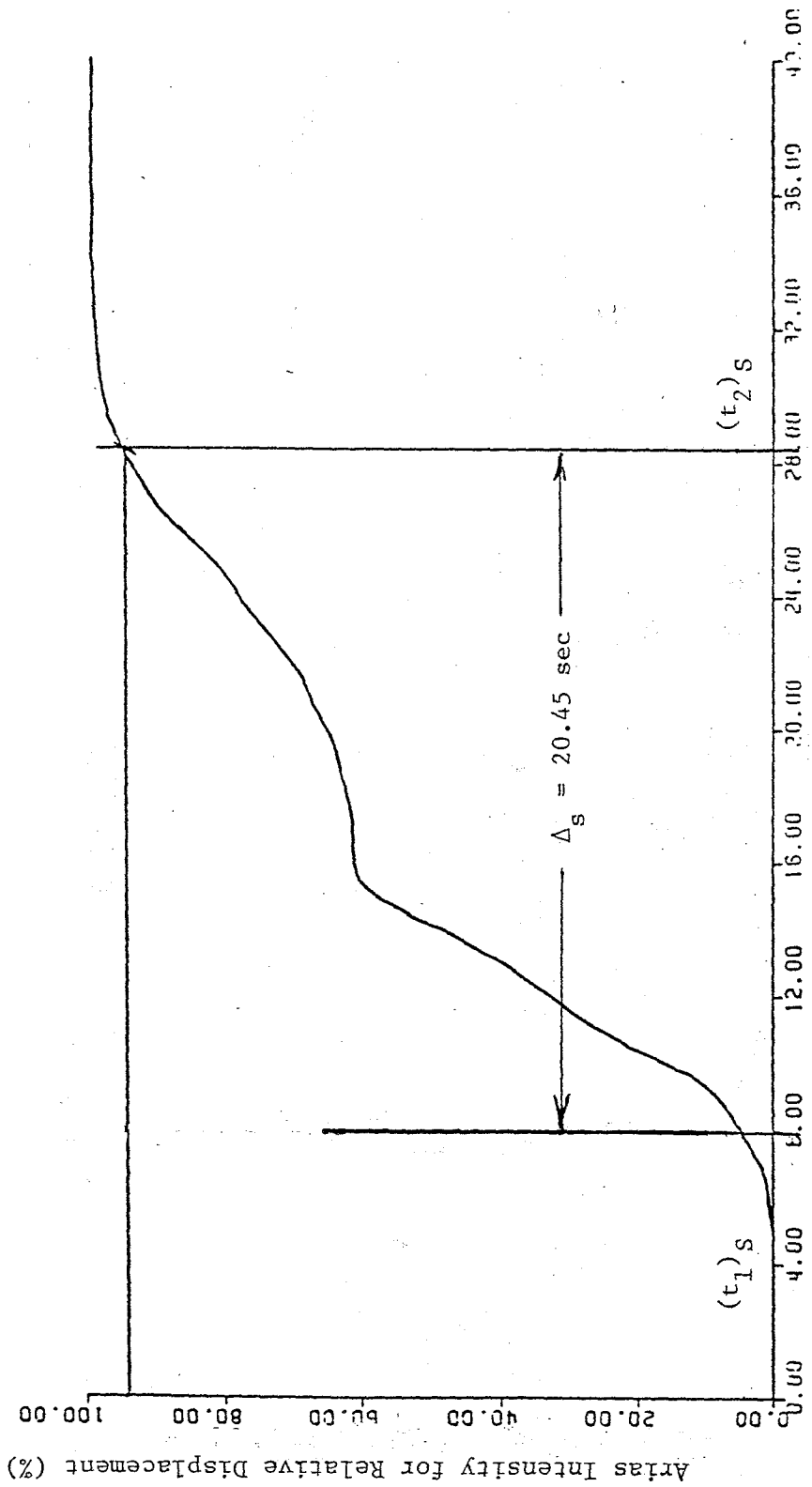

Figure 2.1 Relative Displacement Husid Plot for Millikan Library, N90E Component. During the 1971 San Fernando Earthquake, Showing Duration of Strong Structural Response

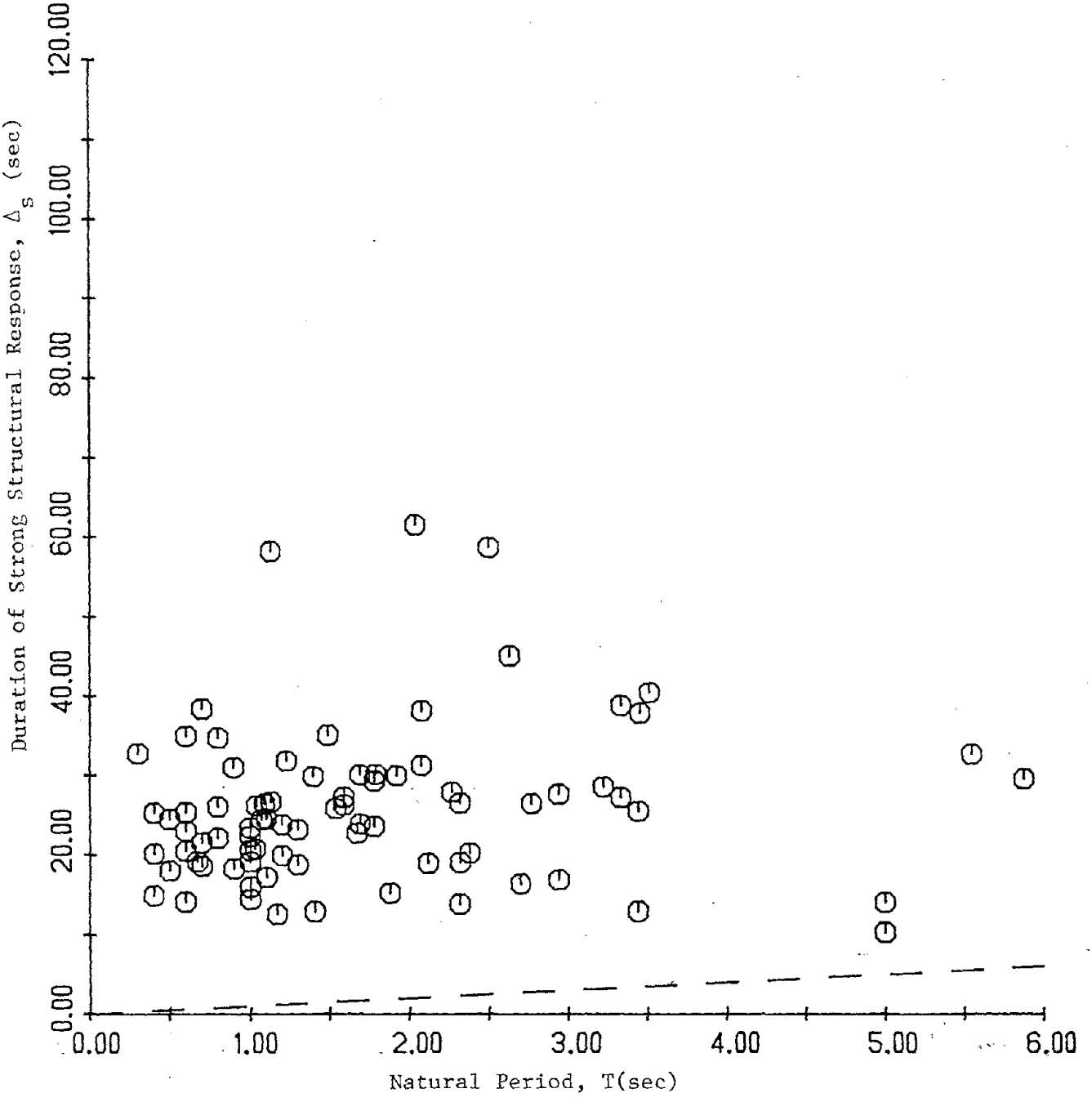

Figure 2.2 Duration of Strong Structural Response versus Natural Period

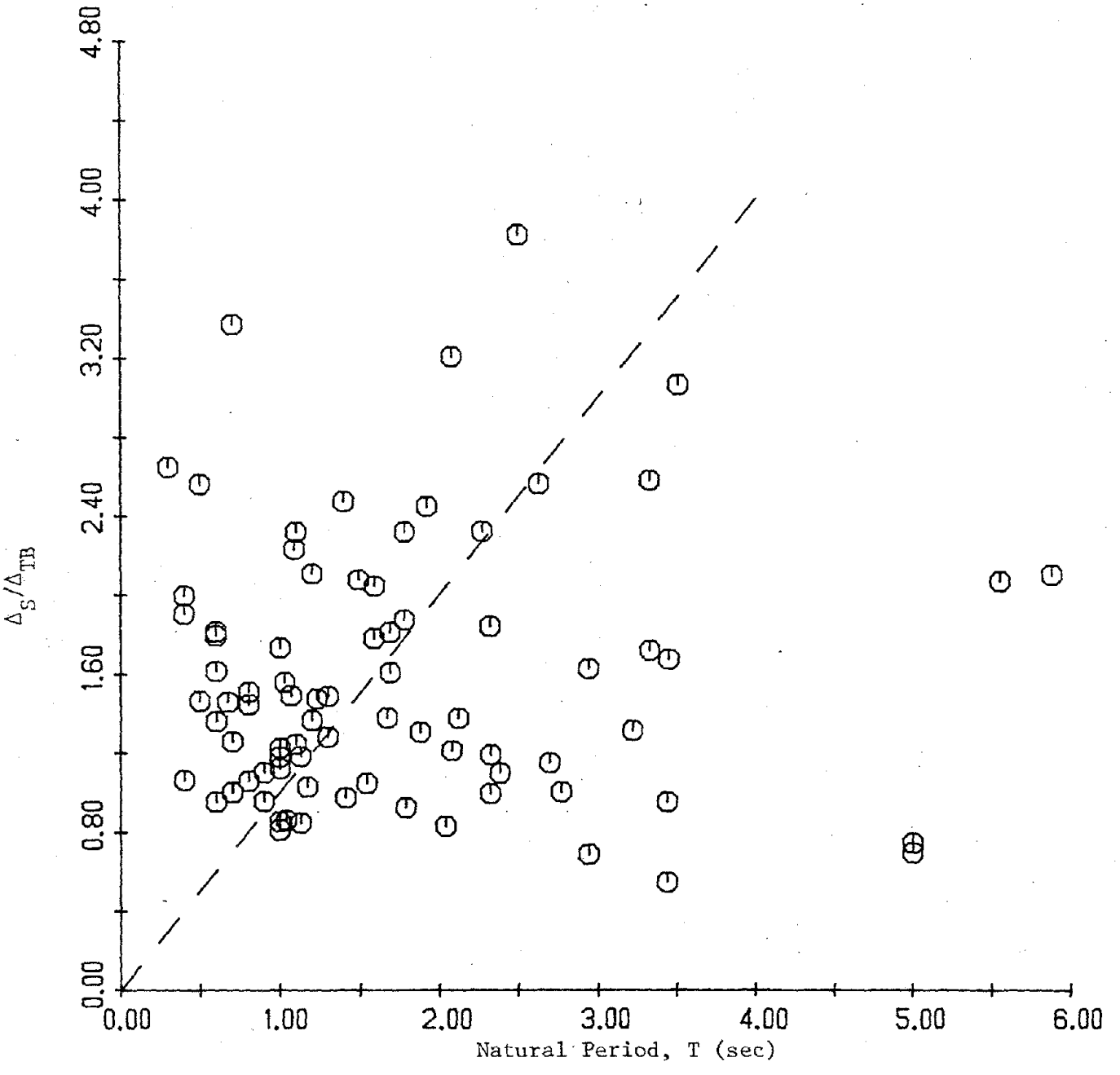

Figure 2.3 Ratio Δ_S/Δ_{TB} Versus Natural Period of Structure

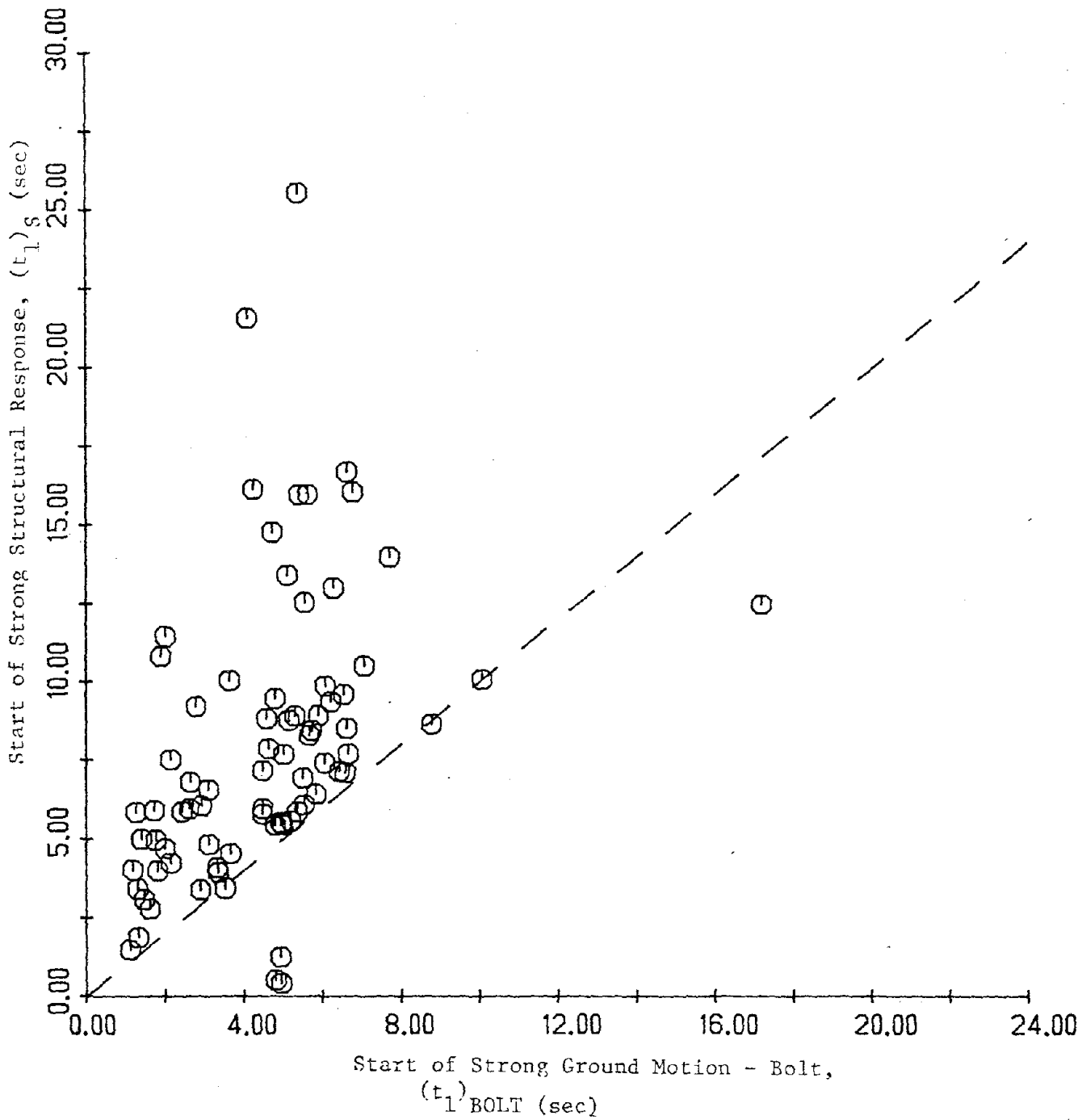

Figure 2.4 Start of Strong Structural Response versus Start of Strong Ground Motion by Bolt's Procedure

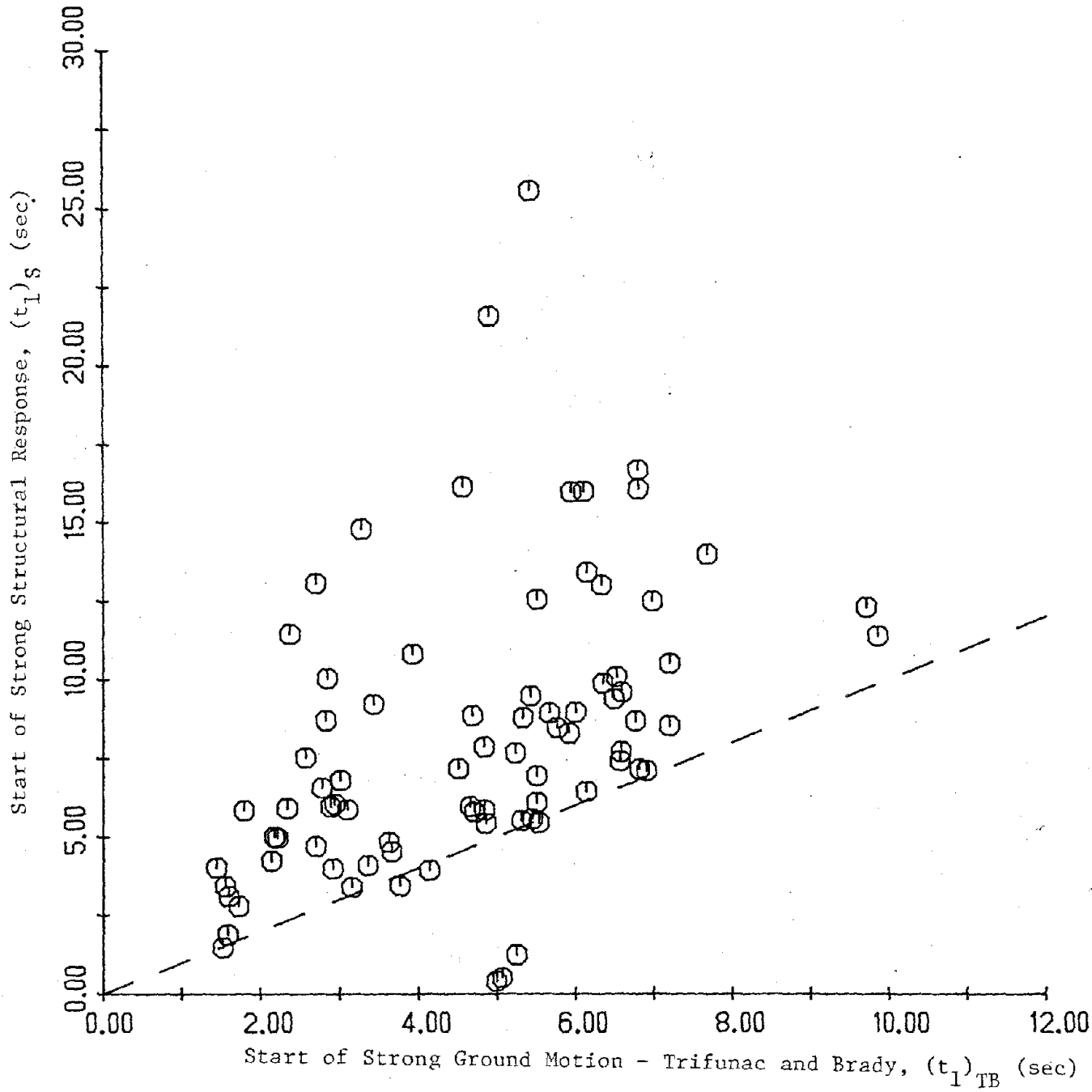

Figure 25 Start of Strong Structural Response versus Start of Ground Motion by Trifunac and Brady's Procedure

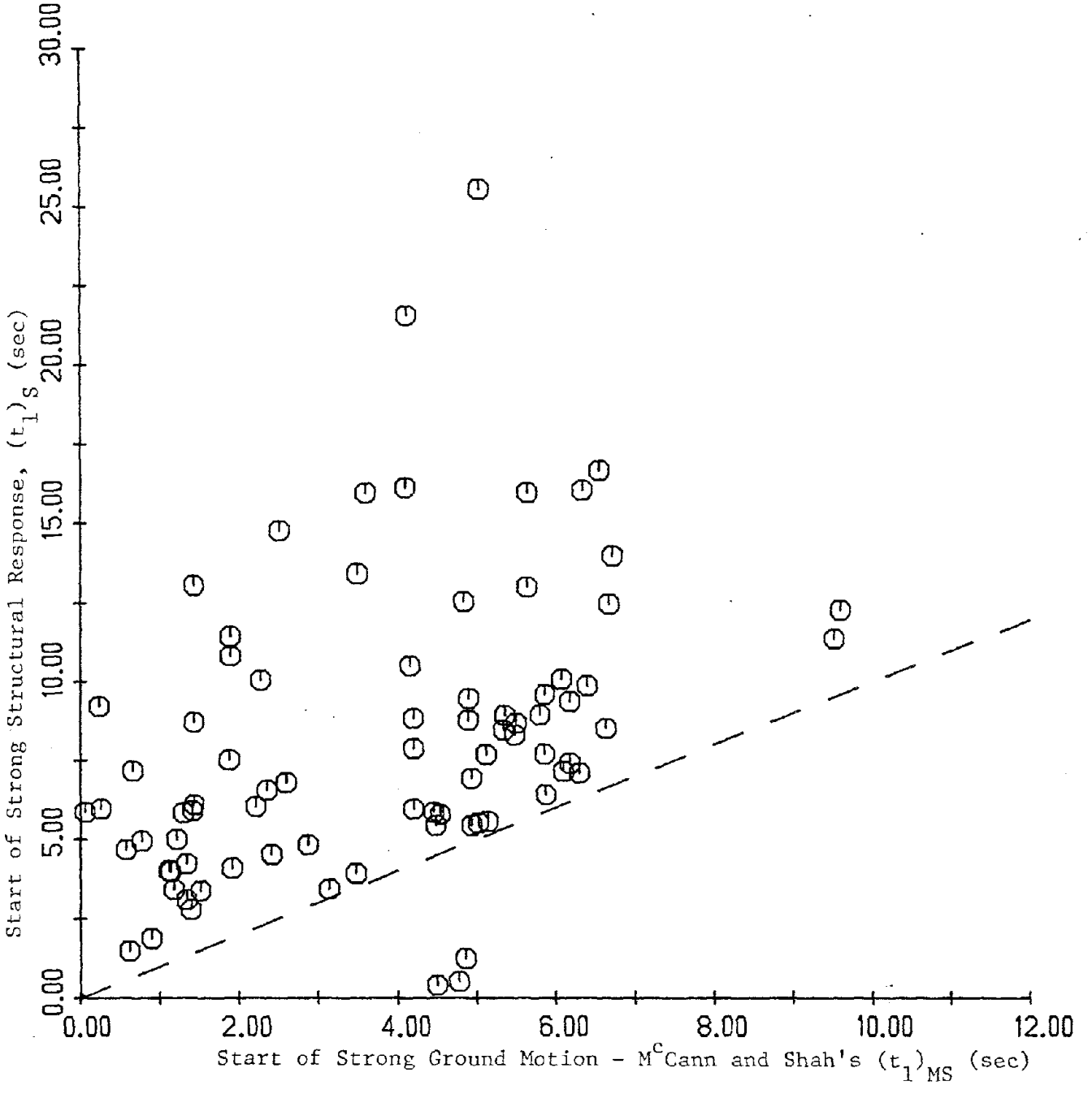

Figure 2.6 Start of Strong Structural Response versus Start of Strong Ground Motion by McCann and Shah's Procedure

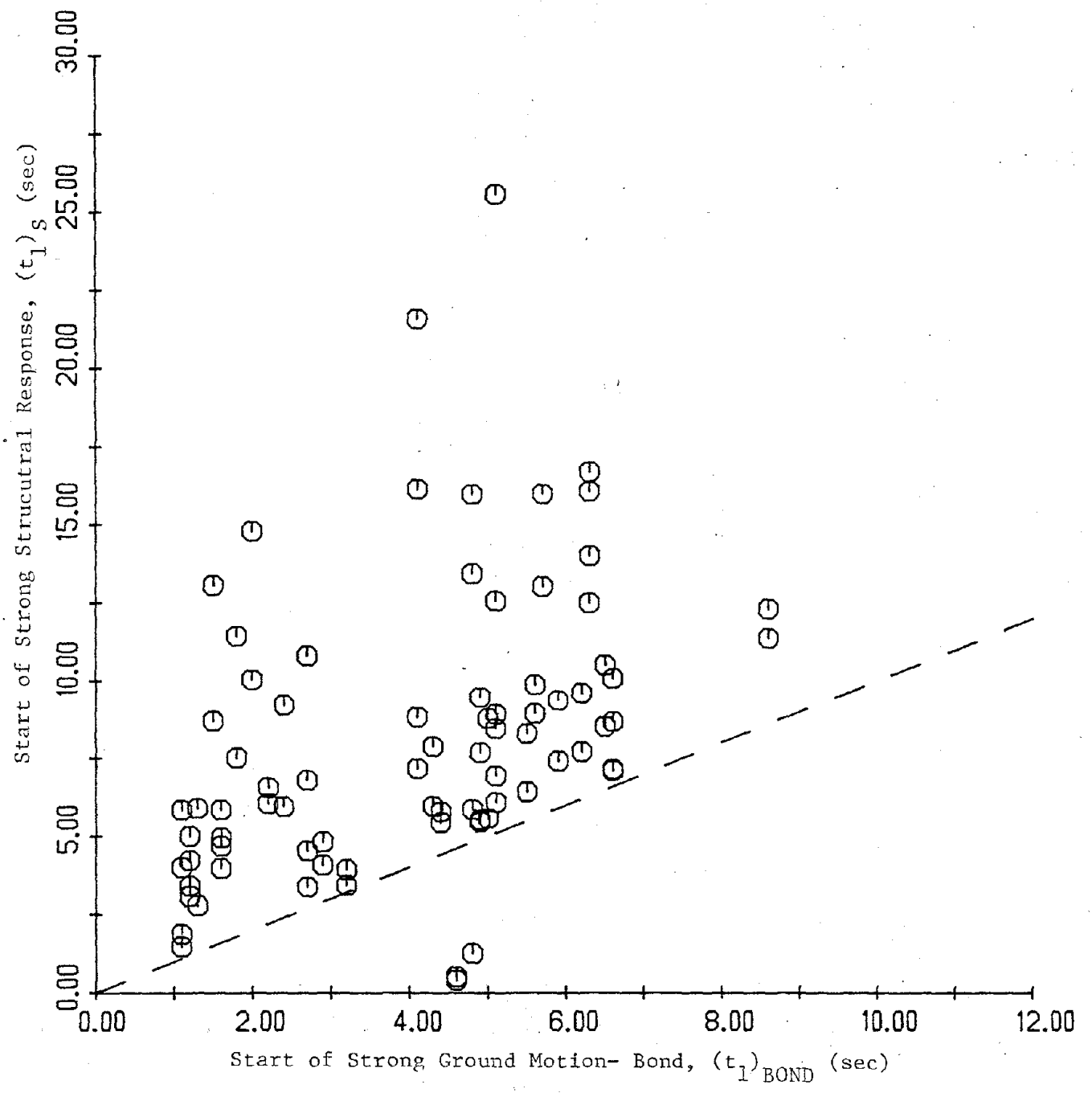

Figure 2.7 Start of Strong Structural Response versus Start of Strong Ground Motion by Bond's Procedure

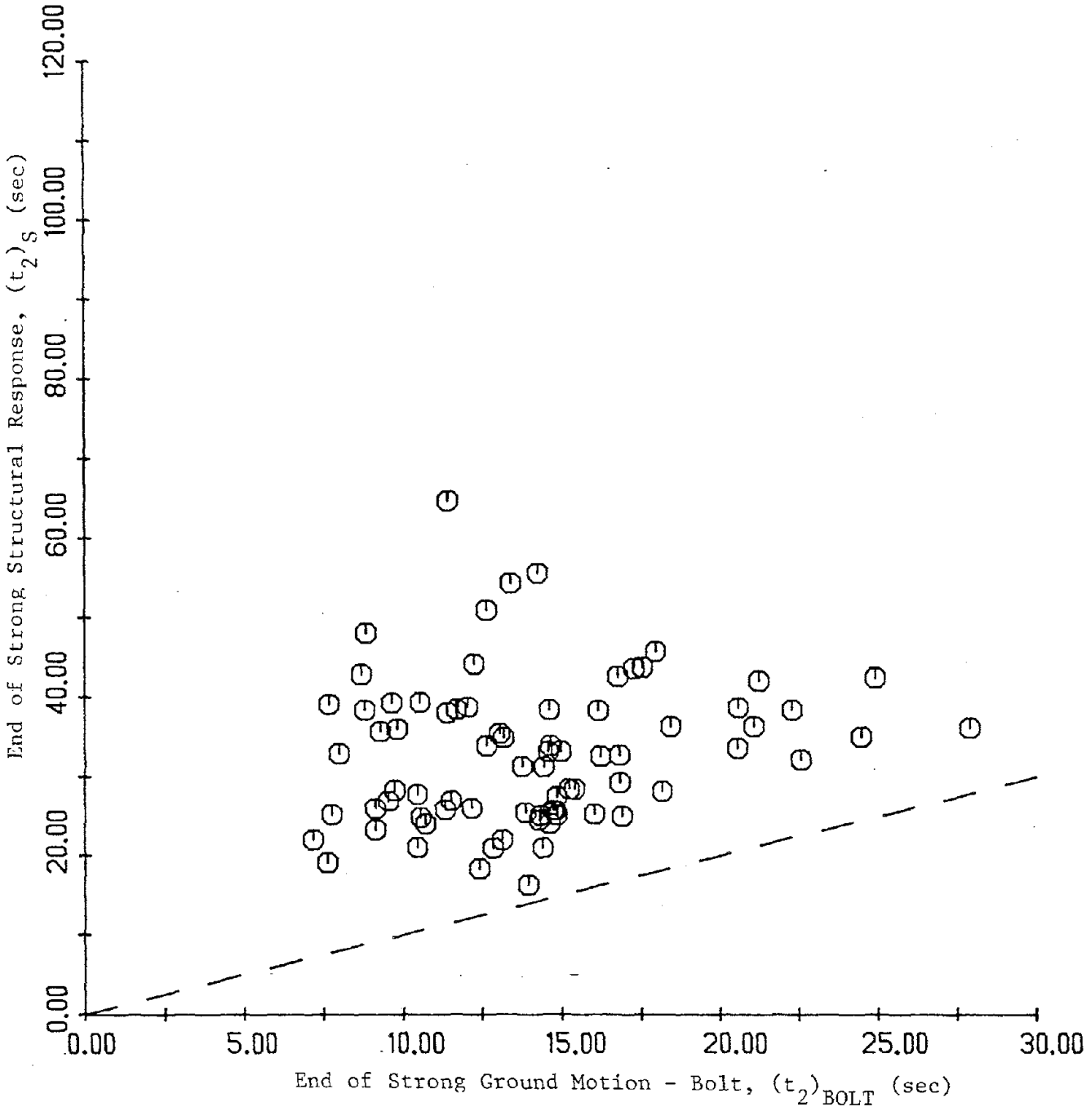

Figure 2.8 End of Strong Structural Response versus End of Strong Ground Motion by Bolt's Procedure

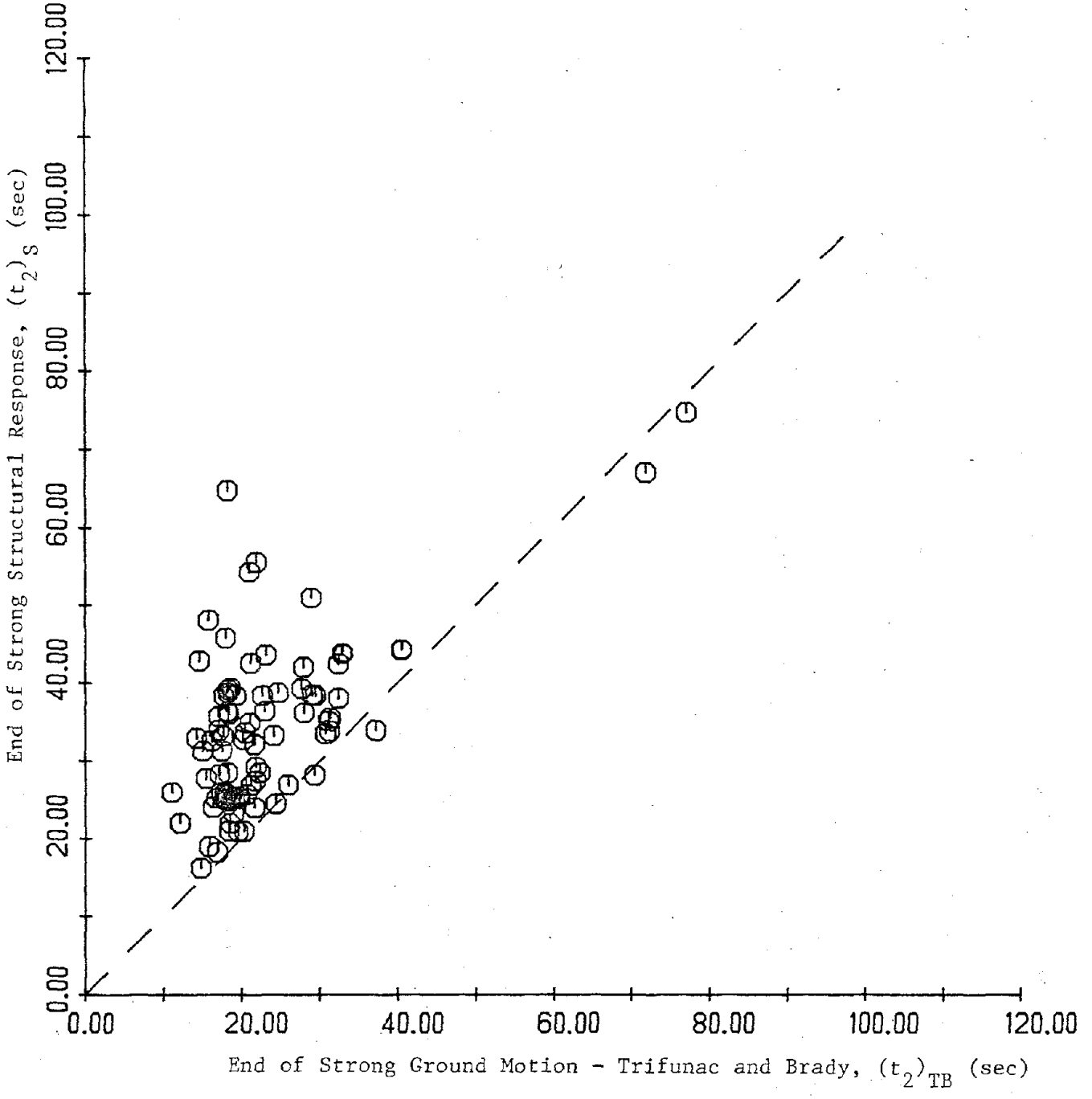

Figure 2.9 End of Strong Structural Response versus End of Strong Ground Motion by Trifunac and Brady's Procedure

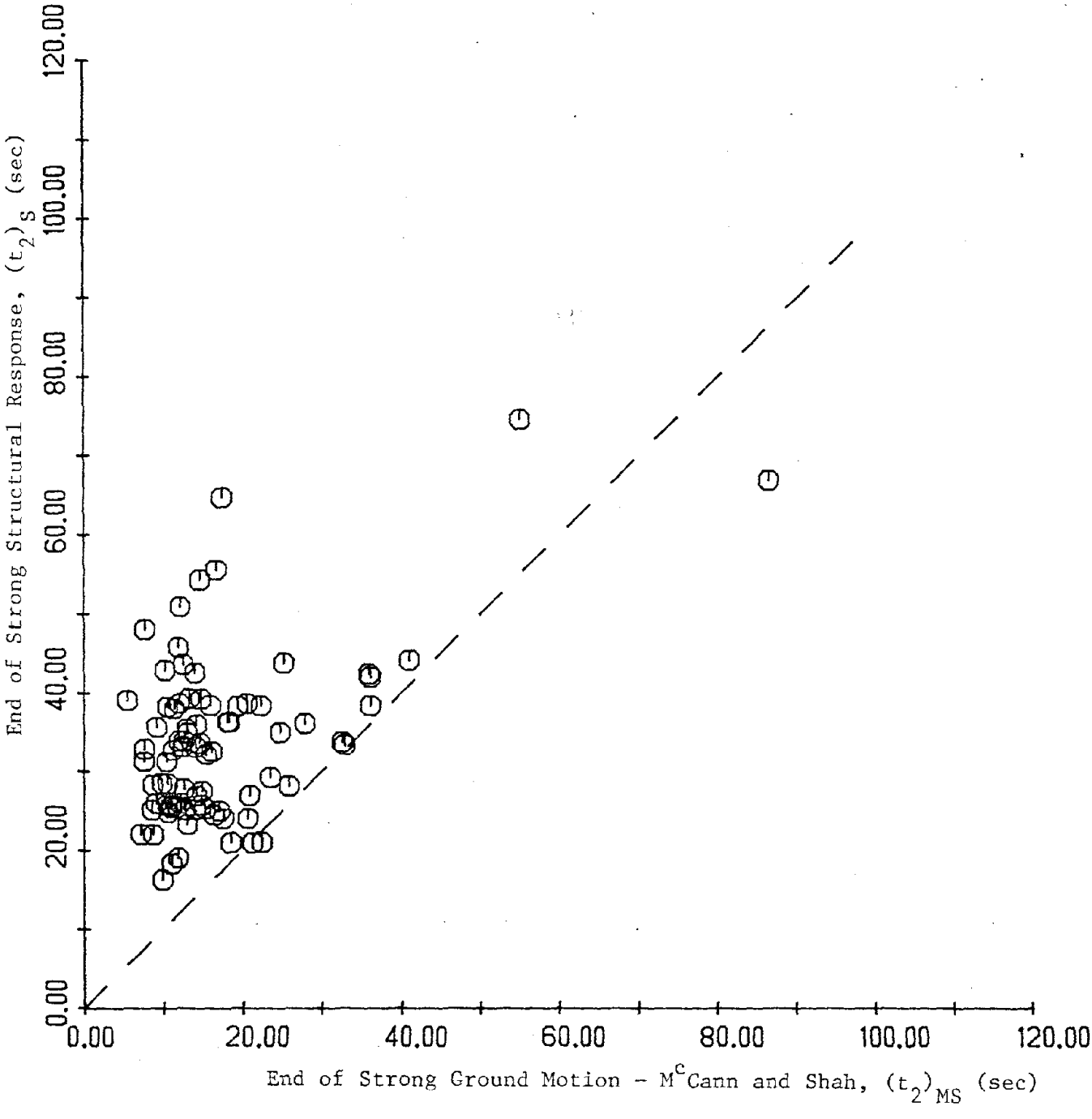

Figure 2.10 End of Strong Structural Response versus End of Strong Ground Motion by M^{c}Cann and Shah's Procedure

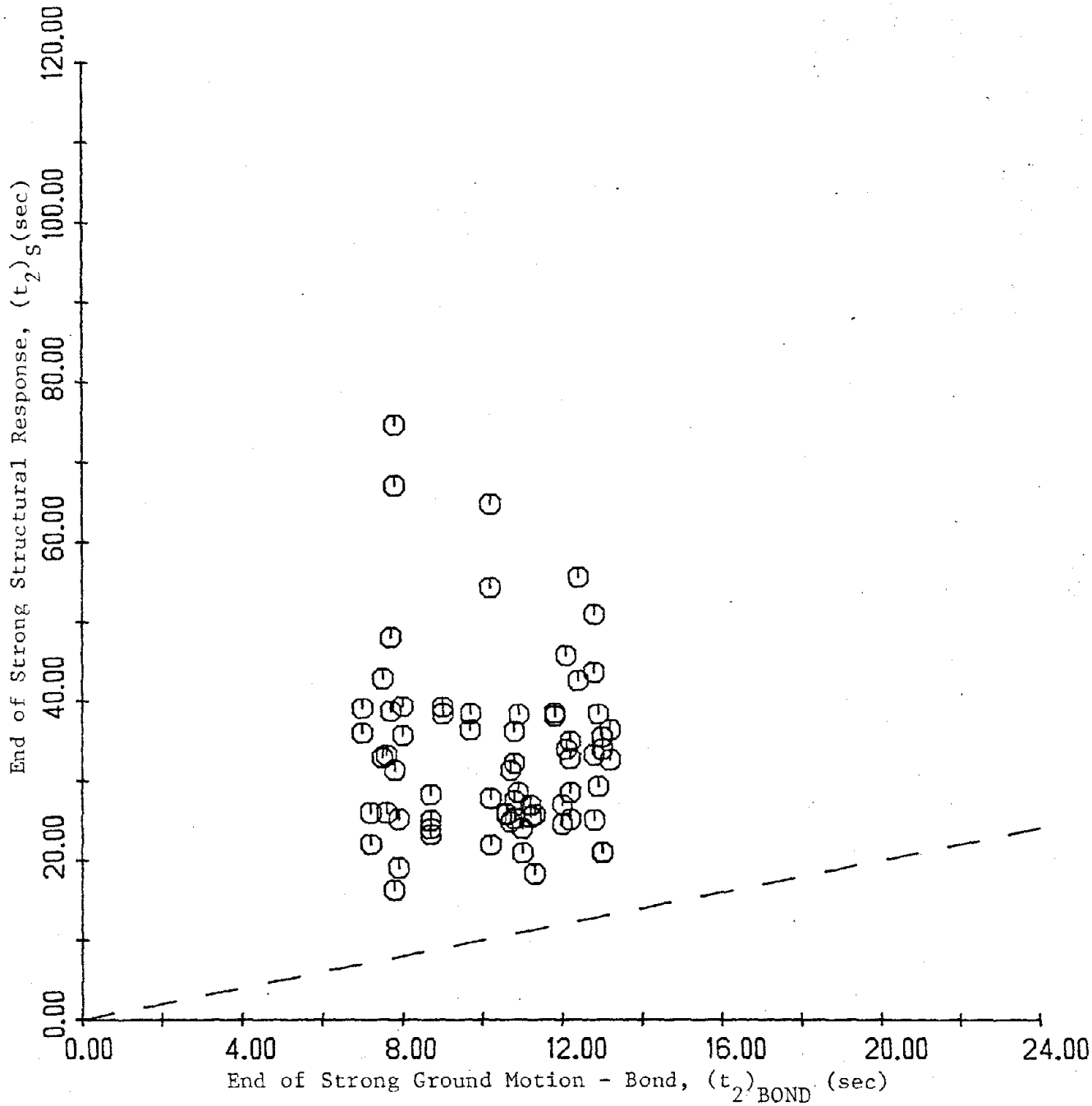

Figure 2.11 End of Strong Structural Response versus End of Strong Ground Motion by Bond's Procedure

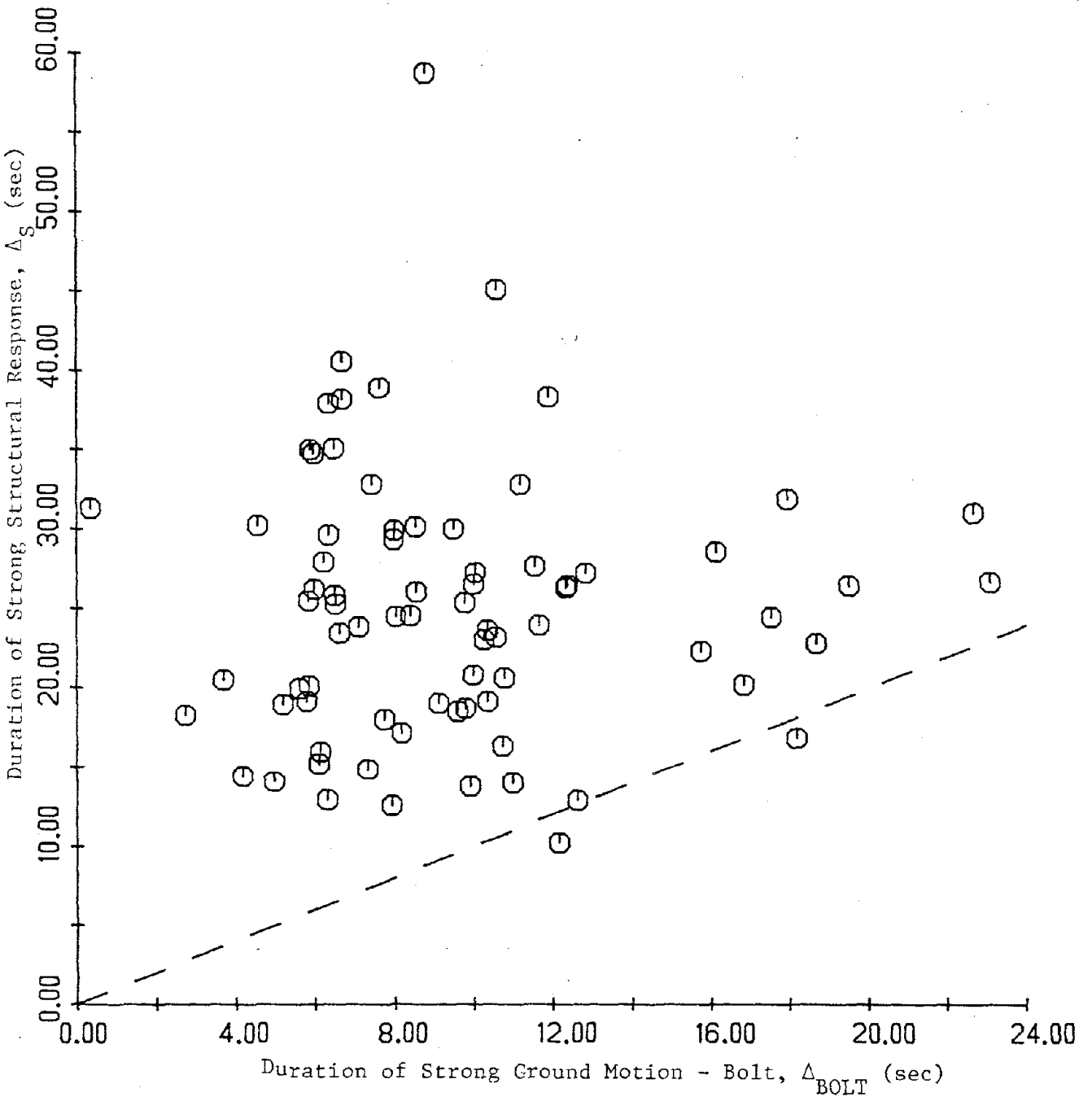

Figure 2.12 Duration of Strong Structural Response versus Duration of Strong Ground Motion by Bolt's Procedure

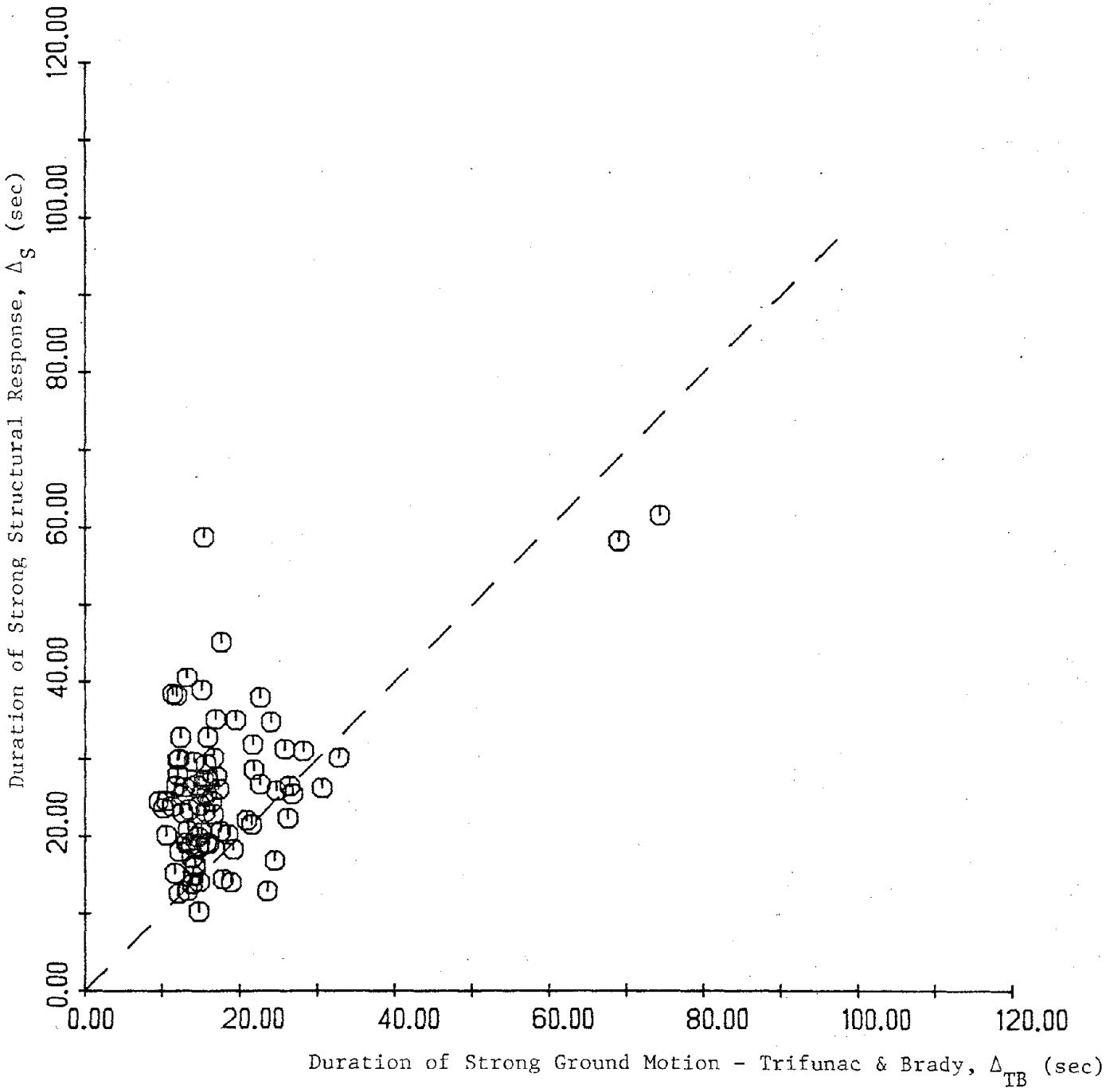

Figure 2.13 Duration of Strong Structural Response versus Duration of Strong Ground Motion by Trifunac and Brady's Procedure

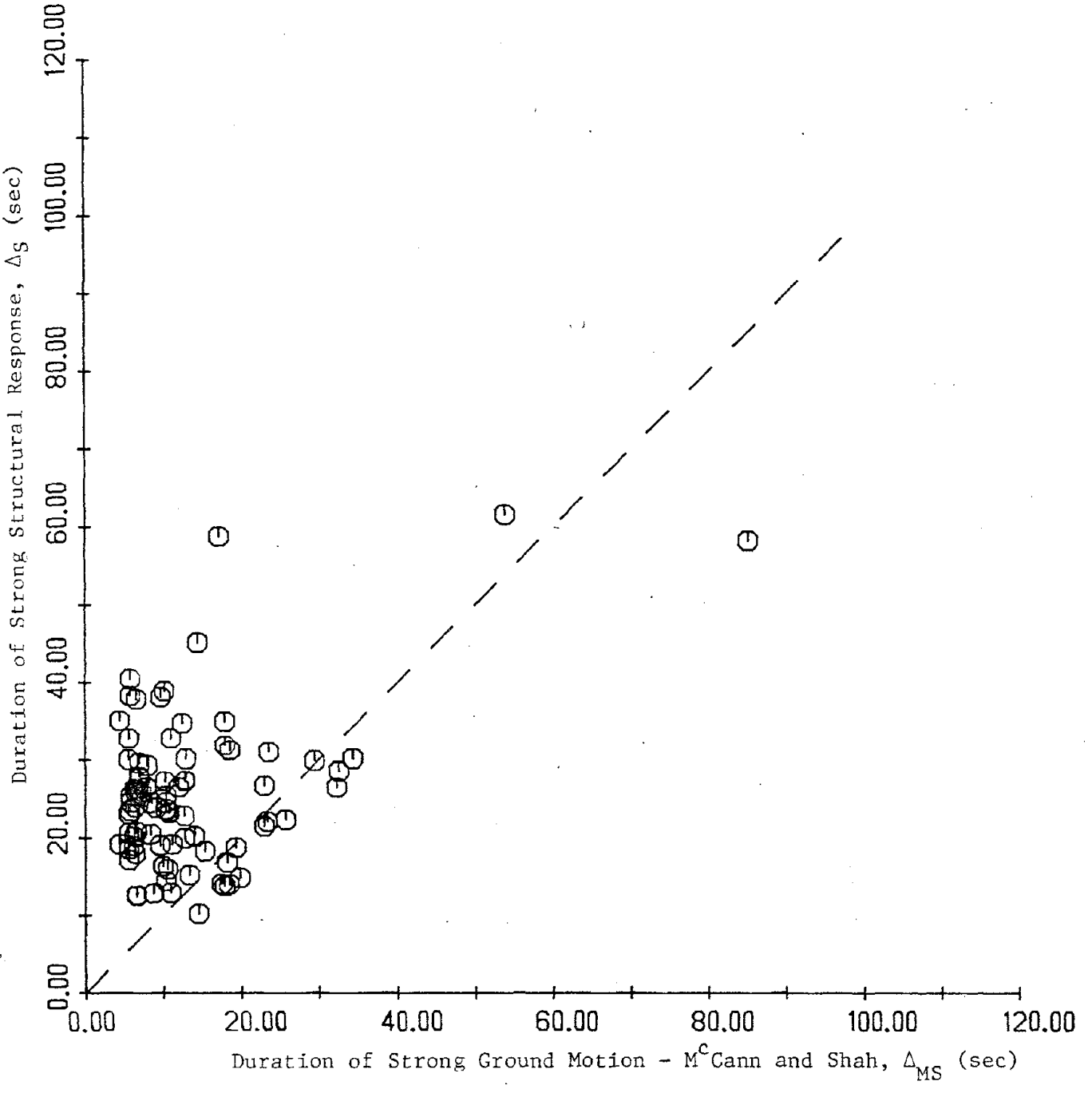

Figure 2.14 Duration of Strong Structural Response versus Duration of Strong Ground Motion by McCann and Shah's Procedure

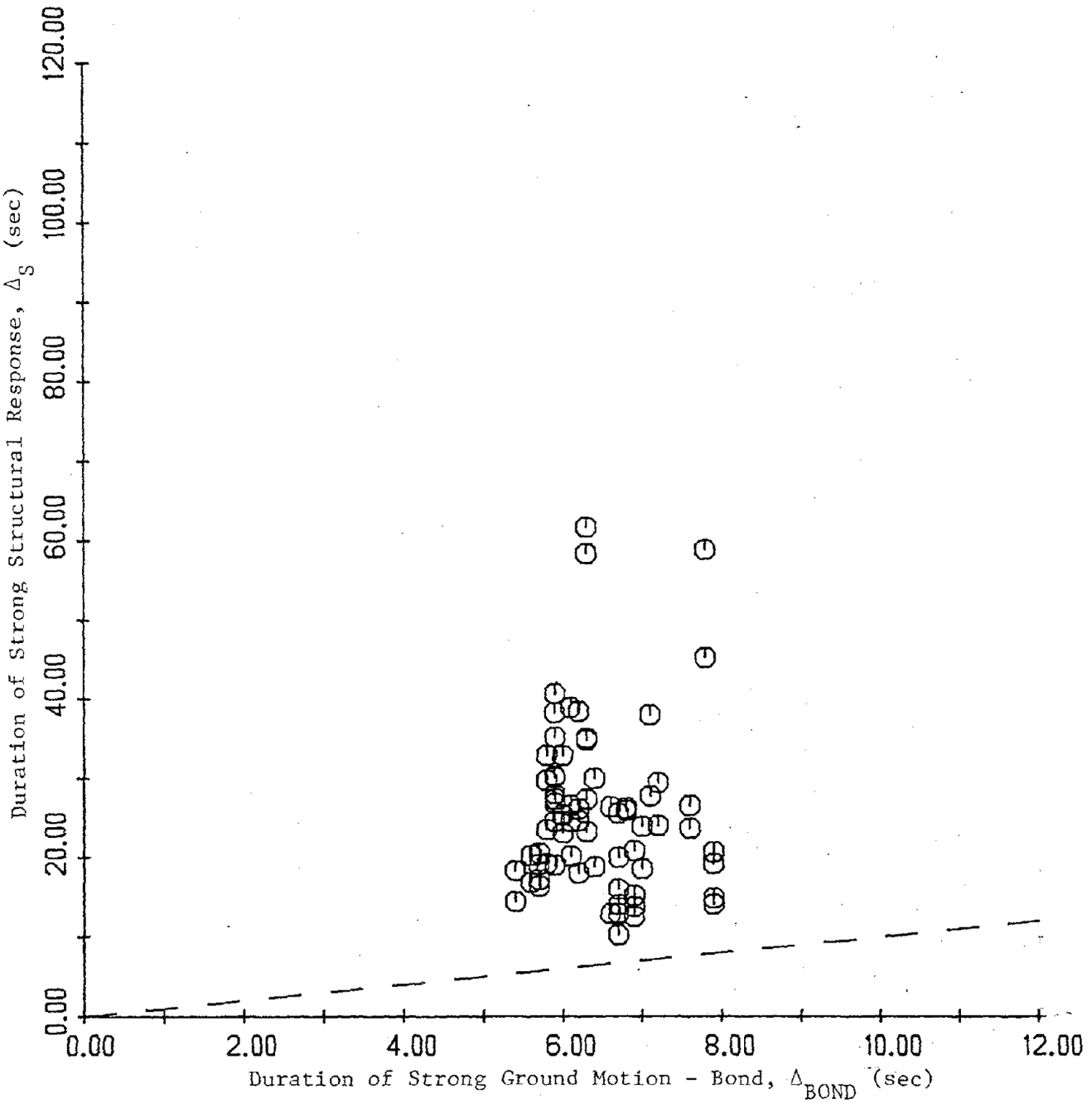

Figure 2.15 Duration of Strong Structural Response versus Duration of Strong Ground Motion of Bond's Procedure

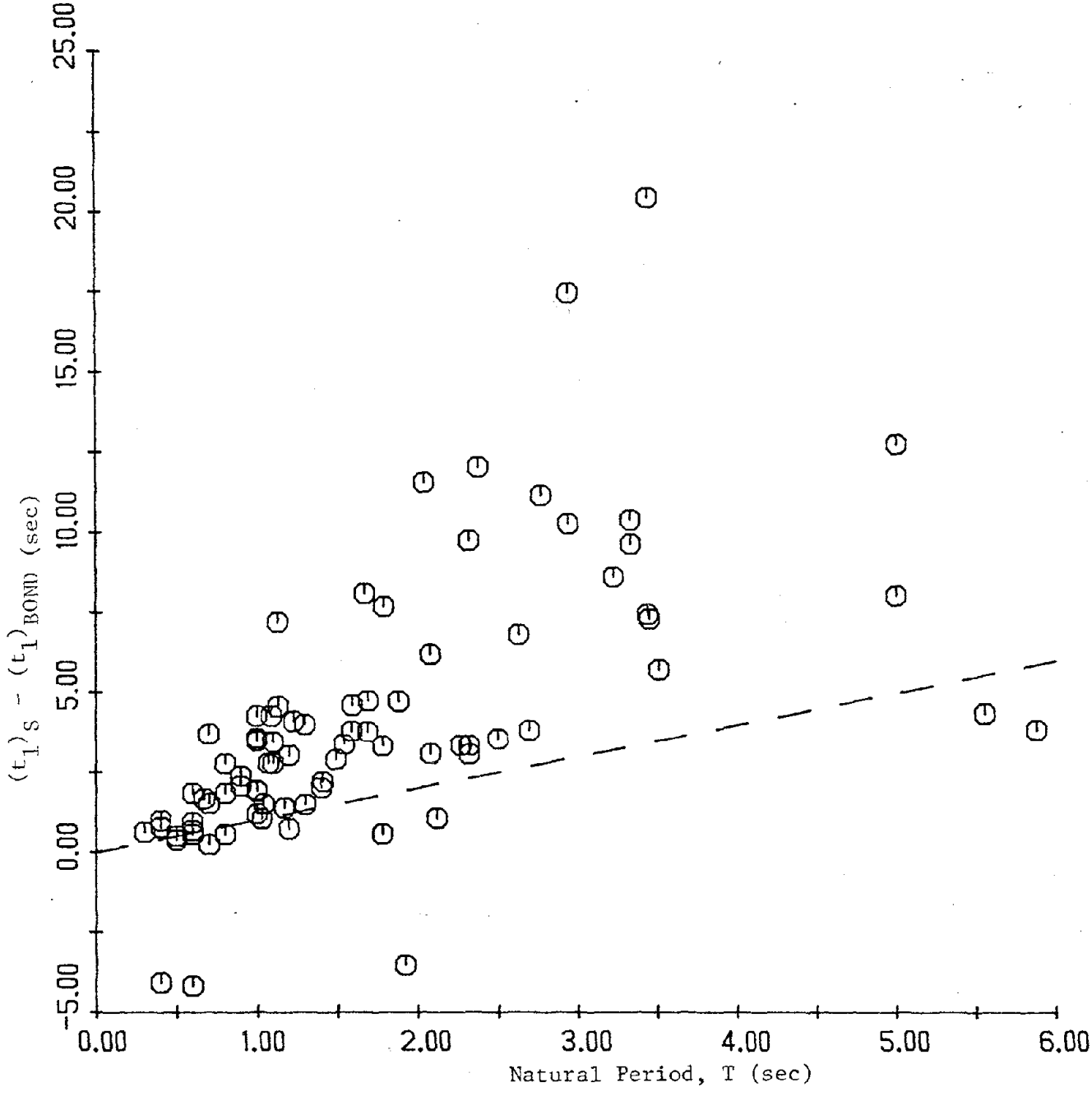

Figure 2.16 Time Lag Between Arrival of S! and Start of Strong Structural Response versus Natural Period of Structure

CHAPTER 3

Degradation of Structural Stiffness

Structural engineers are aware of changes in the basic dynamic characteristics of building which occur during earthquakes. Ogawa and Abe (9) conducted an investigation on more than 200 buildings in the city of Sendai, Japan. The natural periods of the buildings were measured both before and after two major earthquakes which struck the city in 1978. The authors note that the natural periods of the building measured after the earthquake were longer than the natural period of the same structures measured before the earthquake. This indicates a degradation in the effective stiffness of the building during the earthquake.

Mulhern and Maley (8) report similar changes in natural periods for structures which experienced the 1971 San Fernando Earthquake. One of these structures, Cal Tech's Millikan library was the subject of an extensive investigation by Iemura and Jennings (6). They concentrated mainly on the hysteretic response of the structure, and were able to determine the natural frequency and damping as a function of time during the earthquake. They conclude that there was a significant decrease in both the stiffness and damping of the library during the course of the earthquakes.

In this chapter the time period during which this structure stiffness degradation occurs, is determined for a number of structures which recorded the 1971 San Fernando earthquake. This

time period is compared to the time period of strong structural response described in the previous chapter.

3.1 Trilinear Plots

The relative displacement time history of the top floor of the structure Xr(t), was used in determining the degradation of stiffness during the earthquake. To avoid possible long period waves due to errors in digitizing the accelerograms (6,12), the relative displacement time histories were run through a digital band pass filter. In this study, the low frequency cutoff of the filter was taken as half the structures "during earthquake" natural frequency as determined by Mulhern and Maley (8). The high frequency cutoff was set at twice the structure's "pre-earthquake" natural frequency, again from Ref. (8). Shown in Figure 3.1(a) is the filtered relative displacement time history for the N90E component recorded at the Millikan Library during the 1971 San Fernando Earthquake.

The equivalent natural frequency of the structure during the course of the earthquakes is calculated from the filtered relative displacement time history using a moving time window procedure. The equivalent frequency at any particular time is taken as the average frequency for a 5 cycle time window centered about the time point in question. This equivalent natural frequency of Millikan Library for this component is shown in Figure 3.1(b). For the first 5 seconds of recorded motion, the relative displacements

are small, and the equivalent natural frequencies hovers around 1.50 Hz. The stiffness degradation occurs between about 5 and 10 seconds, where there is a fairly linear decrease in the equivalent natural frequency with time. The relative displacement are fairly large during this time period with values up to about 7 cm. After about 10 seconds the equivalent natural frequency has a fairly constant value of 1.0 Hz although the relative displacement are as large as 4 cm.

Figure 3.1(b) is typical of the equivalent frequency versus time plots for structures which experienced stiffness degradation during the San Fernando Earthquake. That is, there is a short time period during which the equivalent frequency is fairly constant, a linear decrease in equivalent frequency during stiffness degradation, followed by a constant post degradation equivalent frequency lower than the pre-degradation equivalent frequency.

Equivalent natural frequency versus time plots were generateed for all the structures listed in Table 1.1. However, many of these structures exhibited no significant structural degradation during the 1971 San Fernando Earthquake. The group of structures listed in Table 3.1 had consistent equivalent natural frequency plots and were selected for the purposes of analysis. The start of stiffness degradation $(t_1)_{DEG}$, and the end of stiffness degradation $(t_2)_{DEG}$ were calculated by fitting the equivalent natural frequency plots with a trilinear curve. The trilinear approximation had linear decrese in frequency for $(t_1)_{DEG}$, $\leq t \leq (t_2)_{DEG}$ and constant frequency for $t \leq (t_1)_{DEG}$, and $t \geq (t_2)_{DEG}$. The trilinear

approximation for the N90E component of Millikan Library is shown in Figure 3.1(b). The values choosen for $(t_1)_{DEG}$, and $(t_2)_{DEG}$ minimized the residual error Er

$$Er = \sum_{j=1}^{n} (\nu(t_j) - \bar{\nu}(t_j))^2 \qquad (9)$$

where $\nu(t_j)$ is the calculated equivalent natural frequency and $\bar{\nu}(t_j)$ is the trilinear approximation.

The start of stiffness degradation $(t_1)_{DEG}$ and the end of stiffness degradation are listed in Table 3.1 for the structures which exhibited consistent equivalent frequency plots. Also listed in Table 3.1 is t_{max}, the time at which the structure's relative displacement is largest

$$|x_r(t_{max})| > |x_r(t)| \qquad \text{for all } t \qquad (10)$$

where $x_r(t)$ is the displacement of the top floor of the structure with respect to its base.

3.2 Comparison Between Stiffness Degradation and Strong Structural Response

The start of stiffness degradation $(t_1)_{DEG}$, is plotted in Figure 3.2 against the start of strong structural response $(t_2)_s$. The vast majority of points fall below the one to one match line indicating that, in general, stiffness degradation begins before strong structural response begins. It is possible that some of the initial stiffness degradation is due to separation between non structural elements such as partitions and the lateral load resisting system at fairly low relative displacement levels.

The end of stiffness degradation $(t_2)_{DEG}$ is plotted in Figure 3.3 against the time of maximum relative displacement, t_{max}. Note that the points tend to follow the one to one match line indicating that, in general, stiffness degradation ends when the maximum relative displacement is largest. That is, after the maximum realtive displacement has occurred, relative displacements less than the maximum value do not seem to produce damage or degradation of either the structural or nonstructural elements.

TABLE 3.1

Start and End of Stiffness Degradation and Time of Maximum Relative Displacement

CalTech Number	Direction	$(t_1)_{DEG}$ (sec)	$(t_2)_{DEG}$ (sec)	t_{max} (sec)
C048	N00W	3.40	12.45	14.90
C048	S90W	2.95	8.55	12.80
D062	S52W	3.10	7.20	8.00
E075	N90E	2.95	24.55	14.80
G108	N90E	5.45	9.90	10.00
I131	N40W	5.05	10.90	9.80
J145	S00W	2.70	15.35	13.30
J145	S90W	3.60	11.15	14.10
M180	S90W	3.40	3.90	18.00
N192	N29E	4.90	16.45	17.20
N192	N61W	3.85	24.20	9.50
O199	N62W	6.80	11.60	9.90
P217	S00W	2.15	10.10	5.20
P217	N90E	3.05	7.75	10.10
Q233	S12W	4.25	13.70	20.20
R244	N53W	10.15	12.95	11.90
R246	SOUTH	6.30	14.05	16.40
R246	EAST	7.00	11.75	12.50
S255	N08E	3.05	7.95	5.30
S255	N82W	2.70	11.55	14.60
S258	N29E	7.60	11.35	14.50

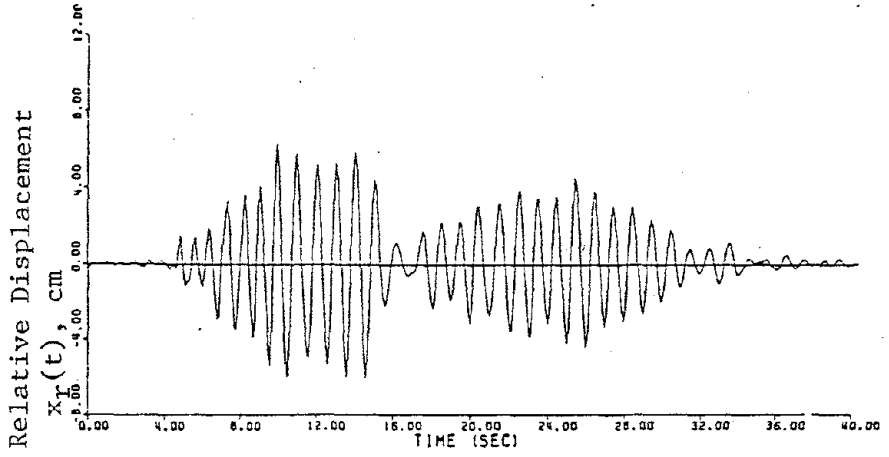

(a) Relative Displacement versus Time

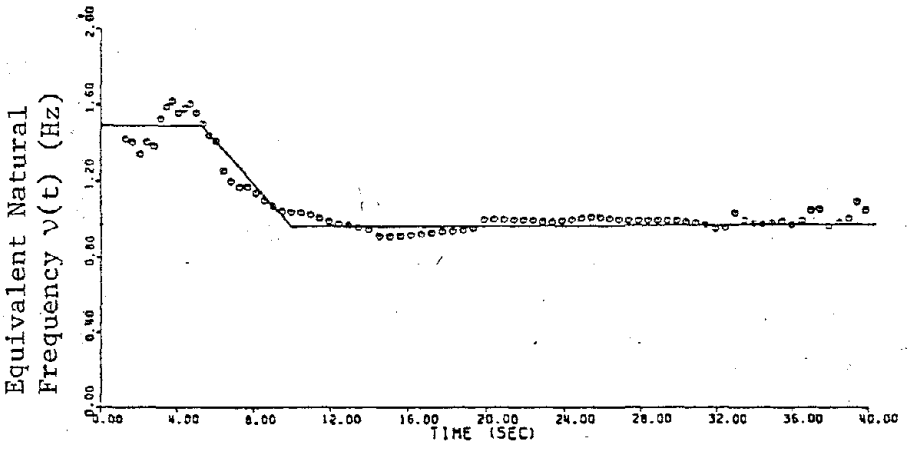

(b) Equivalent Natural Frequency versus Time

Figure 3.1 Plots for N90E Component of Millikan Library

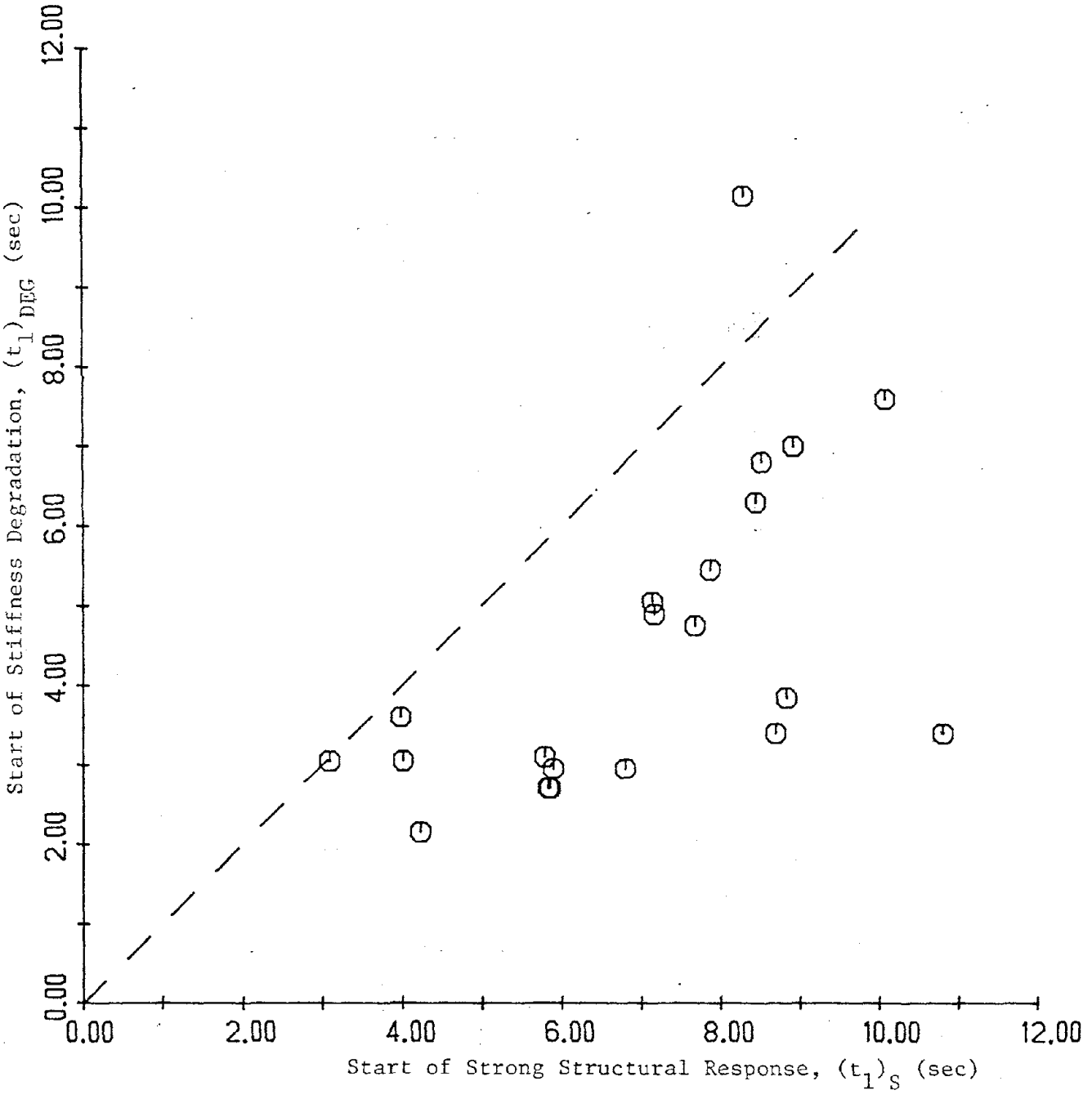

Figure 3.2 Start of Stiffness Degradation versus Start of Strong Structural Response

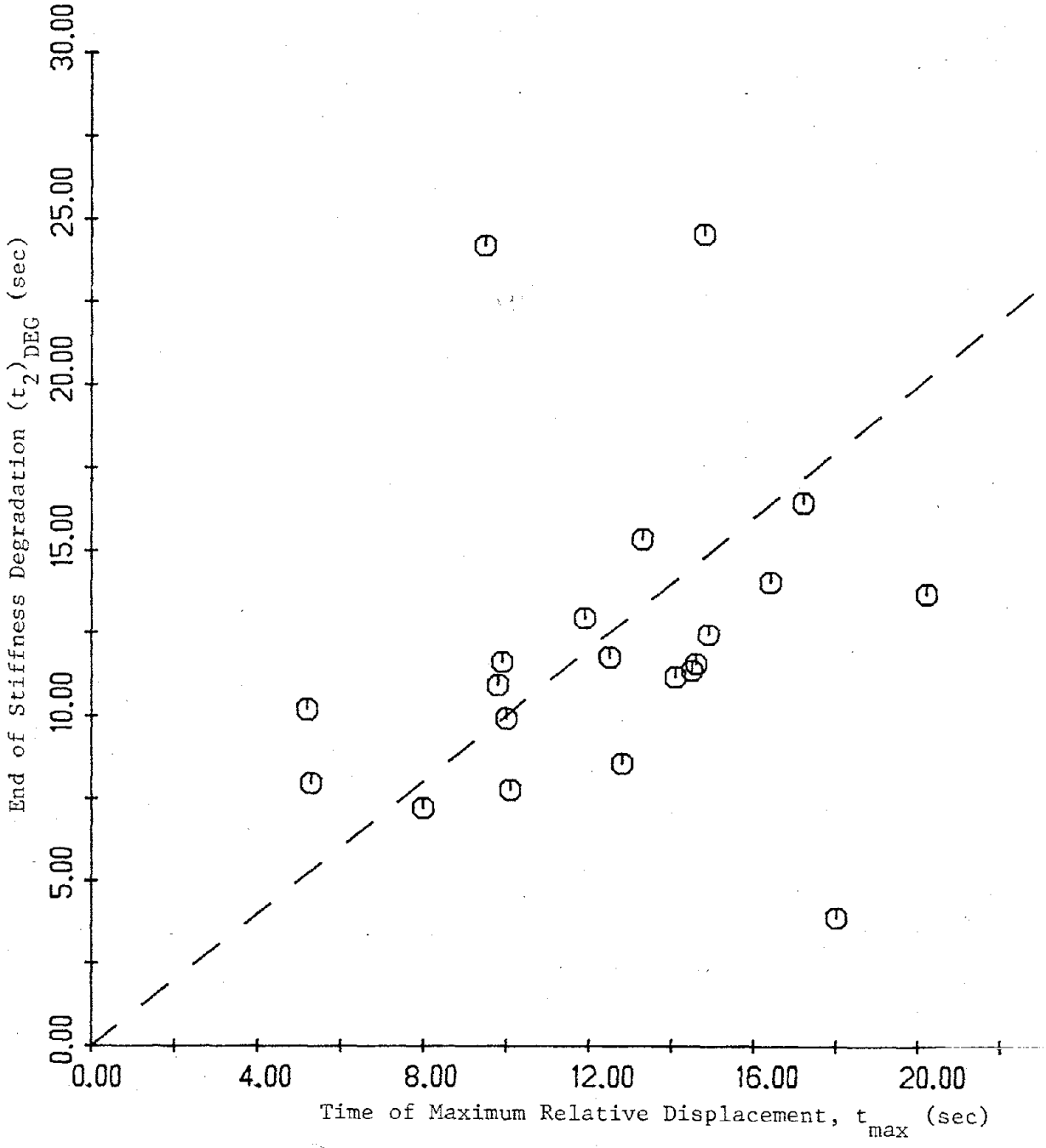

Figure 3.3 End of Stiffness Degradation versus Time of Maximum Relative Displacement

CHAPTER 4

Summary and Conclusions

Durations of strong ground motion at various sites during the 1971 San Fernando Earthquake as defined by Bolt, Trifunac and Brady, M^{C}Cann and Shah, and Bond were compared. Using any of the above methods, the duration of strong ground motion for one of the horizontal components at a site is about equal to the duration for the other horizontal component at the same site. The start of strong ground motion by the four procedures are generally within a second of two of each other. In general, the duration of strong ground motion by Trifunac and Brady procedure, Δ_{TB} is longer than the duration of strong ground motion by M^{C}Cann and Shah's procedure, Δ_{MS}, which in turn is longer than that by Bond's procedure. There was no apparent trend for Bolt's duration, Δ_{BOLT}. This is likely due to the fact that Bolt's duration procedure takes into consideration the amplitude of ground acceleration. Δ_{BOLT} equals zero if the maximum ground acceleration is less than 5% of gravity.

A duration of strong structural response was established using a Trifunac and Brady type procedure. Specifically, the duration of strong structural response was defined as the time required for the Husid plot of the relative displacement at the top floor with respect to its base, to increase from 5% to 95% of its final value. A comparison between ground motion durations and duration of strong structural response indicates that strong

structural response begins after the start of strong ground motion. In addition, strong ground motion ends before the end of strong structural response. However, the match between ground motion duration and structural response duration is a function of the structures natural period. For shorter period structure, T < 2 sec, strong structural response begins about 2 seconds after the start of strong ground motion. For many long period structures, strong structural response begins after the end of strong ground motion. That is, for shorter period structures, the start of strong ground motion by any of the four methods is a fairly good estimate for the start of strong structural response. For longer period structures, none of the four ground motion procedures matches well the time period during which strong structural response occurs. This could very well be due to the fact that the ground motion durations are based on ground acceleration whereas the response of longer period building is more closely related to ground velocities.

The time periods during which stiffness degradation occurred in a group of structures which experienced the 1971 San Fernando Earthquake were determined by plotting equivalent natural frequencies versus time. It was shown that stiffness degradation generally begins before the start of strong structural response. It is possible that some of the initial stiffness degradation is due to separation between structural and non-structural elements at fairly low relative displacement levels. It was also shown that the stiffness degradation generally stops after the maximum relative displacement occurs.

Appendix: References

1. Arias, A., "A Measure of Earthquake Intensity", Seismic Design for Nuclear Power Plants, Robert Hansen, Editor, Massachusetts Institute of Technology Press, Cambridge, Massuchetts, 1969.

2. Bolt, B.A., "Duration of Strong Ground Motions", Proceedings of the Fifth World Conference on Earthquake Engineering, Rome, 1973, pp. 1305-1313.

3. Bond, W.E., R. Dobry and M.J. O'Rourke, A Study of the Engineering Characteristics of the 1971 San Fernando Earthquake Records Using Time Domain Techniques, Report CE-80-1, Department of Civil Engineering, Rensselaer Polytechnic Institute, Troy, NY, June, 1980.

4. Dobry, R., I.M. Idriss and E. Ng, "Characteristics of Horizontal Components of Strong Motion Earthquake Records", Bulletin of the Seismological Society of America, Vol. 68, No. 5, October 1978, pp. 1487-1520.

5. Husid, R., "Gravity Effects on the Earthquake Response of Yielding Structures", Report of Earthquake Engineering Research Laboratory, California Institute of Technology, Pasadena, California, 1967.

6. Iemura, H., and P.C. Jennings, "Hysteretic Response of a Nine-Story Reinforced Concrete Building", Earthquake Engineering and Structural Dynamics, Vol. 13, 1974, pp. 183-201.

7. McCann, M.W., Jr. and H.C. Shah, "Determining Strong-Motion Duration of Earthquakes", Bulletin of the Seismological Society of America, Vol. 69, No. 4, August 1979, pp. 1253-1265.

8. Mulhern, M.R. and R.P. Maley, "Building Period Measurements Before, During and After the San Fernando Earthquake", San Fernando Earthquake of February 9, 1971, United States Department of Commerce, Vol. 1, Part B., pp. 725-733.

9. Ogawa, J. and Abe, Y., "The Stiffness Degradation of Actual

Buildings caused by a Severe Earthquake", Int. Conf. on Eng. for Protection from Natural Hazards, Asian Inst. of Technology 1980.

10. Seed, H.B., I.M. Idriss, F. Makdaki, and N. Bannerji, "Representation of Irregular Stress Time Histories by Equivalent Uniform Stress Series in Liquefaction Analyses", Report Earthquake Research Center 75-29, College of Engineering, University of California, Berkeley, CA, 1975.

11. Trifunac, M.D. and A.G. Brady, "A Study of the Duration of Strong Earthquake Ground Motion", Bulletin of the Seismological Society of America, Vol. 65, No. 3, June, 1975.

12. Udwadia, F.E., and M.D. Trifunac, "Time and Amplitude Dependent Response of Structures", Earthquake Engineering and Structural Dynamics, Vol. 2, 1974, pp. 359-378.

13. Vanmarcke, E.H. and S.P. Lai, "Strong-Motion Duration of Earthquakes", Evolution of Seismic Safety of Buildings, Report #10, Department of Civil Engineering, Massachusetts Institute of Technology, Cambridge, MA, July 1977.